Thermomechanics of a heterogeneous fluctuating chain

Tianxiang Su, Prashant K. Purohit.*

Department of Mechanical Engineering and Applied Mechanics, University of Pennsylvania, Philadelphia, PA 19104.

Abstract

In this paper we present a theory to efficiently calculate the thermo-mechanical properties of fluctuating heterogeneous rods and chains. The central problem is to evaluate the partition function and free energy of a general heterogeneous chain under the assumption that its energy can be expressed as a quadratic function in the kinematic variables that characterize the configurations of the chain. We analyze the effects of various types of boundary conditions on the fluctuations of the rods and chains and show that our results are in agreement with recent work on homogeneous rods. The results for the heterogeneous chains are verified through Monte Carlo simulations. Finally, we consider a special heterogeneous chain with only two bending moduli and use it as a model to interpret experiments on partially unfolded protein oligomers.

Key words: heterogeneous wormlike chain, force-extension behavior, protein forced unfolding, Monte Carlo simulation.

1. Introduction

Single molecule mechanical experiments on rod-like biomolecules, such as, DNA and actin have for long been interpreted using a model of a homogeneous fluctuating elastic rod (Bustamante et al., 1994; Marko and Siggia, 1995; Odijk, 1995; Nelson, 2008). However, advanced single molecule techniques are now capable of probing the structure and properties of macromolecules at length scales of a few nanometers. At these length scales it is no longer sufficient to think of the molecules as having homogeneous mechanical properties. In fact, several recent studies have revealed the remarkable effects of the heterogeneous properties of some biopolymers on their conformations as well as their mechanical behaviors (Popov and Tkachenko, 2007; Moukhtar et al., 2007). For example, heterogeneous mechanical properties are encountered in partially unfolded protein oligomers in atomic force microscopy (Su and Purohit, 2009). Sequence specific mechanical properties of DNA are already well known and it has been suggested that DNA binding proteins can sense these heterogeneities, making them biologically significant (Hogan et al., 1983; Hagerman, 1988; Zhang and Crothers, 2003). Also, it has been noted that localized softening in DNA can have significant influence on looping probabilities which ultimately affect genetic activity (Purohit and Nelson, 2006;

*Corresponding author.
Email address: purohit@seas.upenn.edu (Prashant K. Purohit.)

Wilson et al., 2007). These examples show that heterogeneous mechanical properties have been observed in experiments on biomolecules and that even at relatively large length scale, they can have significant biological consequences which the homogeneous models cannot capture. They motivate us to examine the consequences of heterogeneity through detailed mathematical models.

A simple way of introducing heterogeneity in polymer models is to group monomers into hydrophilic and hydrophobic types as has been done in some recent articles (Geissler and Shakhnovich, 2002; Jarkova et al., 2005). Another model which accounts for heterogeneity is the two-state worm-like-chain model of Ahsan et al. (1998), which reduces to the fluctuating rod model in the low force limit, and to the Ising model at high forces (Ahsan et al., 1998). The approach in this paper is different from these methods in that we allow the bending modulus $K_b(s)$ of our fluctuating rod to vary as an arbitrary function of the arc length s. We first evaluate the partition function of the rod in a constant force and constant temperature ensemble, and then compute the free energy and a host of other thermal and mechanical properties of the rod. The results are verified through Monte Carlo simulations. A special case of our model is one in which there are only two possible values of the bending modulus K_I and K_{II} along the chain. We call this the 'special heterogeneous chain' and use it to interpret the force-extension data from the forced unfolding experiments on protein oligomers.

Our method also allows us to determine the consequences of constraints imposed on the rod. In particular, we can determine the force-extension relation and the magnitude of transverse fluctuations under different types of boundary conditions. Boundary conditions siginificantly affect the fluctuations if the length of the rod is comparable or shorter than its persistence length (Seol et al., 2007). The effect of boundary conditions on the fluctuations of homogeneous rods has been analyzed only recently by a few authors (Purohit et al., 2008). In this paper we apply three different boundary conditions on the rod and compare our results with those of Purohit et al. (2008) for homogeneous rods and find excellent agreement. The method used in this paper is more general than that of Purohit et al. (2008) which is based on the equipartition theorem and can only be applied to homogeneous rods.

This paper is organized as follows. We first use the equipartition theorem to derive some general results for heterogeneous chains with arbitrary boundary conditions. We then demonstrate a method for calculating the thermo-mechanical properties of chains and rods under three different boundary conditions. We use Monte Carlo simulations and comparisons with earlier work to show that our method gives accurate results. Finally, we apply our method to interpret data from force-extension experiments on the protein ubiquitin.

2. Description of the Model

We study the thermo-mechanical properties of a fluctuating heterogeneous elastic chain in this paper. A theory for a 2D chain is presented first and then the results are generalized to 3D.

Let $\{\hat{X}, \hat{Y}\}$ be a standard reference dyad in 2D space, an N-segment chain with one end fixed at the origin and the other end subjected to an external force $\vec{F} = F\hat{X}$ is fluctuating around its equilibrium state. As shown in Fig. 1, each configuration of the chain is characterized by N tangent angles θ_i, formed by the segments with respect to the $\hat{X}$ axis. We

assume that (1) the length of the segment l is a constant independent of the applied force, and therefore, the chain is inextensible with contour length being $L = Nl$; (2) the chain is untwistable [1]. Therefore, the elastic energy of the chain arises only from bending and it is given by:

$$E = \sum_{i=1}^{N-1} \frac{K_i}{2l}(\theta_{i+1} - \theta_i)^2, \tag{1}$$

where K_i is the bending modulus that varies along the heterogeneous chain. A continuum version of this energy is obtained by taking the limit as $l \to 0$ and $N \to \infty$ while $Nl = L$ remains fixed and is given by:

$$E_{\text{rod}} = \int_0^L \frac{K(s)}{2}\dot{\theta}(s)^2 ds, \tag{2}$$

where s is the arc length along the rod and $\dot{\theta}$ is the derivative of θ with respect to s.

Up to a quadratic approximation, the Hamiltonian of the chain (or rod in the continuum limit) in a fixed T (temperature in Kelvin) and F (force) ensemble is:

$$\begin{aligned} \beta(E - Fx) &= \int_0^L \frac{\beta K(s)}{2}\dot{\theta}(s)^2 ds - \beta F \int_0^L \cos\theta ds & (3)\\ &\approx \beta \sum_{i=1}^{N-1} \kappa_i(\theta_{i+1} - \theta_i)^2 + \beta f \sum_{i=1}^{N} \theta_i^2 - \beta FL, & (4) \end{aligned}$$

where $\beta = (k_B T)^{-1}$ and k_B is the Boltzmann constant, x is the extension (end-to-end distance projected onto the $\hat{X}$ axis) of the chain and κ_i, f are respectively the bending modulus and the force in energy units:

$$\kappa_i = \frac{K_i}{2l}, \quad f = \frac{Fl}{2}. \tag{5}$$

For a short chain whose contour length L is comparable to its persistence length $\xi_p \sim K/k_B T$ [2], we expect the thermomechanics and the fluctuation of the chain to depend on the boundary conditions. We consider three different boundary conditions in this paper (Fig. 1): (1) hinged-hinged chain: both ends of the chain are hinged on the $\hat{X}$ axis with no moments acting on them; (2) partially clamped chain: one end of the chain is clamped at the origin while the other end, with slope constrained to be zero, is free to have transverse displacement in the Y direction. (3) clamped-clamped chain: both ends of the chain are clamped on the $\hat{X}$ axis. All these three boundary conditions have been realized in experiments using different types of apparatuses (Purohit et al., 2008). Note that for a long chain with $L >> \xi_p$, we expect the thermomechanics of the chain to be insensitive to the boundary conditions.

[1] Although twist may be important in some cases, we neglect it here and focus on (1) the effects of heterogeneity and (2) different boundary conditions. Nelson (2008) gives some explanation about the simplification of neglecting the twisting energy.

[2] Here we define the persistence length ξ_p as $\langle \hat{t}(s_0) \cdot \hat{t}(s_0 + s)\rangle = e^{-s/\xi_p}$, where $\hat{t}$ is the unit tangent vector of the chain. This definition leads to $\xi_p = 2K/k_B T$ for a 2D chain and $\xi_p = K/k_B T$ for a 3D chain (Kulić, 2004)

3. Theory

3.1. Statistical mechanical and thermodynamic description of the chain

For a chain in a fixed temperature T and F ensemble, the partition function is:

$$Z = \sum_{\nu} \exp\left[\, -\beta \left(E_\nu - F x_\nu\right) \right], \tag{6}$$

where the summation is over all the allowed configurations ν, with E_ν and x_ν respectively being the energy and the extension of the chain. From the definition of the partition function (Eq. 6), we get:

$$\langle E - Fx \rangle = \frac{1}{Z} \sum_{\nu} (E_\nu - F x_\nu) \exp\left[\, -\beta \left(E_\nu - F x_\nu\right) \right] = -\left(\frac{\partial \log Z}{\partial \beta} \right)_F, \tag{7}$$

where $\langle A \rangle$ denotes the ensemble average of a quantity A and 'log' denotes the natural logarithm in this paper.

On the other hand, since the Hamiltonian is quadratic in the configuration angles θ_i (Eq. 4), we have the equipartition theorem for a fixed T, F ensemble:

$$\langle E - Fx + FL \rangle = \frac{D}{2} k_B T, \tag{8}$$

where D is the number of degrees of freedom of the system.

Eq. 7 together with Eq. 8 leads to a partial differential equation for the partition function Z:

$$\left(\frac{\partial \log Z}{\partial \beta} \right)_F = -\frac{D}{2\beta} + FL, \tag{9}$$

integrating which we get:

$$\log Z = -\frac{D}{2} \log \beta + FL\beta - W(F), \tag{10}$$

where $W(F)$ is an unknown function of F. Note that Eq. 10 holds for any heterogeneous chain with any boundary condition, and all this information is included in $W(F)$, which is independent of the temperature T. Also, regarding to the units in Eq. 10, we shall see in the later sections (Eq. 34, Eq. 49 and Eq. 59) that $W(F)$ includes D terms of the logarithm of quantities in energy units, which combine with the term $-\frac{D}{2} \log \beta$ in Eq. 10 to make the argument of the 'log' dimensionless.

Using the relation between the partition function Z and the free energy G, we obtain $G(T, F)$ expressed in terms of $W(F)$:

$$G(T, F) = -k_B T \log Z = \frac{D}{2\beta} \log \beta - FL + \frac{W(F)}{\beta}. \tag{11}$$

Eq. 11 shows how the free energy $G(T, F)$ depends on T and F up to an unkown function $W(F)$. Note that $G(T, F)$ is the fundamental quantity for a fixed T, F ensemble because all thermo-mechanical quantities can be derived from it (Callen, 1985). Here, by using

the equipartition theorem, we have been able to deduce a form for $G(T, F)$ in which the dependences on T and F are conveniently decoupled. All thermo-mechanical quantities can now be expressed in terms of $W(F)$. More importantly, we will see that $W(F)$ and its derivative, which we denote as $\Delta(F) = W'(F)$, have clear physical meanings and unlike $G(T, F)$, can be measured directly in a single force-extension experiment.

We derive the thermo-mechanical quantities in terms of $W(F)$ and its derivatives $\Delta(F)$, $\Delta'(F)$ below. The entropy of the chain is given by:

$$S = -\left(\frac{\partial G}{\partial T}\right)_F = \frac{1}{2}Dk_B\,[\,1 + \log(k_BT)\,] - k_BW(F). \tag{12}$$

Eq. 12 shows that the contributions of T and F to the entropy are decoupled.

The extension of the chain is given by a simple formula:

$$\langle x\rangle = -\left(\frac{\partial G}{\partial F}\right)_T = L - k_BT\cdot\Delta(F). \tag{13}$$

where again $\Delta(F)$ is the derivative of $W(F)$: $\Delta(F) = W'(F)$. Note that as a special case, the well-known formula for the 2D hinged-hinged homogeneous wormlike chain has exactly the form of Eq. 13, with $\Delta(F)$ given by (Purohit et al., 2008):

$$\Delta_{\text{homo}}(F) = \frac{1}{4}\left[\frac{L}{\sqrt{KF}}\coth\left(\frac{FL}{\sqrt{KF}}\right) - \frac{1}{F}\right]. \tag{14}$$

It is interesting that the simple expression Eq. 13 holds for any general chain, with all the complexity of the heterogeneity and boundary information appearing only in the function $\Delta(F)$. Also note that the dependence on T of $\langle x\rangle$ is the same for all chains with any heterogeneity and boundary conditions (Eq. 13). In fact, this conclusion is true for all the thermo-mechanical quantities shown below.

More importantly, Eq. 13 implies that the unknown function $\Delta(F)$ is actually the 'shrinking' of the chain $(L-\langle x\rangle)$ scaled by the inverse of the thermal energy $\beta = (k_BT)^{-1}$. Therefore, this unkown function of F can be measured in a single force-extension experiment and its independence of T can also be tested. Further, to reveal the physical meaning of $W(F)$, we integrate Eq. 13 with respect to F once to get:

$$k_BT\cdot W(F) = LF - \int\langle x\rangle dF. \tag{15}$$

The integral on the right-hand-side of Eq. 15 is the complementary energy of the chain (Fig. 2), therefore, $k_BT\cdot W(F)$ is the difference between LF and the complementary energy, which corresponds to the shaded area beneath the force-extension curve shown in Fig. 2 and can be measured in a single force-extension experiment. Once $W(F)$ and $\Delta(F)$ are measured, all the other thermo-mechanical properties of the chain are known, as we will show below. We note that $k_BT\cdot W(F)$ is not exactly the energy stored in the chain, which is $\int Fdx = Fx - \int xdF$. We also note that $W(F)$ can only be measured up to a constant because of the indefinite integral in Eq. 15. However, this constant will not appear in $\Delta(F)$, which is the derivative of $W(F)$.

The variance of extension is related to the derivative of $\langle x \rangle$ with respect to F (Callen, 1985) and it is given by:

$$\langle (\Delta x)^2 \rangle = k_B T \left(\frac{\partial \langle x \rangle}{\partial F} \right)_T = -(k_B T)^2 \cdot \Delta'(F), \tag{16}$$

where Eq. 13 has been used. Eq. 16 implies that the variance of extension always scales as T^2. Note that $\langle (\Delta x)^2 \rangle$ is non-negative, so $\Delta'(F) \leq 0$ and therefore $\Delta(F)$ is a decreasing function, as it should be, because it is the 'shrinking' of a chain under a force F.

Using basic thermodynamic relations (Callen, 1985), the average energy of the chain and its variance can also be expressed in term of $\Delta(F)$ and $\Delta'(F)$:

$$\langle E \rangle = \langle E - Fx \rangle + F\langle x \rangle = k_B T \left[\frac{D}{2} - F \cdot \Delta(F) \right], \tag{17}$$

$$\langle (\Delta E)^2 \rangle = -\left(\frac{\partial \langle E \rangle}{\partial \beta} \right)_{F/T} = (k_B T)^2 \left[\frac{1}{2} D - 2F \cdot \Delta(F) - F^2 \cdot \Delta'(F) \right]. \tag{18}$$

thermo-mechanical properties, such as heat capacity C_F, coefficient of thermal expansion α as well as the isothermal extensibility χ, are second derivatives of the free energy G (Callen, 1985). Using Eq. 11, Eq. 12 and Eq. 13, we get:

$$C_F = T \left(\frac{\partial S}{\partial T} \right)_F = \frac{k_B D}{2}, \tag{19}$$

$$\alpha = \frac{1}{\langle x \rangle} \left(\frac{\partial \langle x \rangle}{\partial T} \right)_F = \frac{-k_B \cdot \Delta(F)}{\langle x \rangle} = \frac{1}{T\,[\,1 - \beta L / \Delta(F)\,]}, \tag{20}$$

$$\chi = \frac{1}{\langle x \rangle} \left(\frac{\partial \langle x \rangle}{\partial F} \right)_T = \frac{-k_B T \cdot \Delta'(F)}{\langle x \rangle} = \frac{\Delta'(F)}{\Delta(F) - \beta L}. \tag{21}$$

Note that the heat capacity C_F is a constant independent of both T and F.

From Eq. 20, we find that the inverse of the coefficient of thermal expansion is linear with respect to T:

$$\frac{1}{\alpha} = T - \frac{L}{k_B \cdot \Delta(F)}. \tag{22}$$

This can be tested in a single thermal expansion experiment with constant force F acting at the end of the chain. We further note that the condition $\langle x \rangle \in [0, L]$ on Eq. 13 leads to $\alpha \leq 0$ in Eq. 22, which means the chain shrinks in response to an increase in temperature.

Moreover, Eq. 13 combined with Eq. 20 suggests that if one does a force-extension experiment and a thermal expansion experiment, one should find the results of the two experiments related by:

$$\frac{\langle x \rangle}{L} = \frac{1}{1 - \alpha T}, \tag{23}$$

with both sides evaluated at the same F and T. Note that this relation (Eq. 23) does not invlove the unknown function $W(F)$ and therefore it is not affected by the heterogeneity and boundary condition of the chain. It (Eq. 23) implies that a stiffer chain, which has a larger value of $\langle x \rangle$/L, will have a smaller value of $|\alpha|$ and therefore is less sensitive to the change

of temperature. In addition, Eq. 23 constitutes a falsifiable prediction of our theory and can be tested in experiments.

To sum up, we have been able to express the thermo-mechanical properties for any heterogeneous chain with any boundary conditions in terms of a single-variable unknown function $W(F)$, instead of $G(T,F)$ and $Z(T,F)$. Moreover, unlike $G(T,F)$ and $Z(T,F)$, $W(F)$ and its derivative $\Delta(F)$ have clear physical meanings and are easy to measure in a single force-extension experiment using Eq. 13[3]. Therefore, by doing a single experiment, one can get all the thermo-mechanical properties for the chain, without assuming the chain is homogeneous and regardless of the type of boundary condition applied. Finally, we note that the results in this section hold for the 2D chains as well as the 3D chains except that the prefactor in Eq. 14 should be replaced by 1/2 in 3D case (see Kulić (2004) and also the discussions on the relation between 2D and 3D chains in the latter section 3.6).

3.2. Hinged-hinged 2D chain

As has been shown in the previous section, all the thermo-mechanical quantities can be expressed in terms of $W(F)$ and its derivatives. In what follows we obtain analytic expressions for this function for a general 2D heterogeneous chain with hinged-hinged boundary conditions.

For a hinged-hinged chain (Fig. 1(a)), one end of the chain is fixed at the origin while the other end is constrained on the $\hat{X}$ aixs, in other words, the Y coordinate of the end of the chain is 0. This position constraint expressed in terms of the configuration tangent angles θ_i is:

$$g(\theta_i) = \frac{1}{l} \cdot \int_0^L \sin\theta \, ds \approx \sum_{i=1}^{N} \theta_i = 0. \tag{24}$$

g is called the constraint function and it has been nondimensionalized. We will use the Laplace method (Carrier et al., 2005) below to evaluate the partition function, so it is sufficient to expand $\sin\theta$ up to the first order in Eq. 24 (see the discussions below and also footnote 4).

The partition function (Eq. 6), which sums over all the allowed configurations determined by the constraint function $g(\theta_i)$ (Eq. 24), can be written in an integral form:

$$Z = \int_{-\infty}^{+\infty} \cdots \int_{-\infty}^{+\infty} \exp\left[\, -\beta(E - Fx) \,\right] \delta(g) \, d\vec{\theta}, \tag{25}$$

where $d\vec{\theta} = [\, d\theta_1 \, d\theta_2 \cdots d\theta_N \,]$ and $\delta(g)$ is the Dirac delta function acting on $g(\theta_i)$.

Note that the exact integral limits should be $\theta_i = \pm\pi$. But, noticing that the term $\beta(E - Fx)$ reaches its minimum value $(-\beta FL)$ at $\theta_i \equiv 0$, we have applied the Laplace

[3]Note that the shrinking $\Delta(F)$ can be measured directly while the energy $W(F)$ can be measured only up to an undetermined constant. But, from Eq. 13 to Eq. 21, we see that most of the thermo-mechanical quantities are expressed only in terms of $\Delta(F)$, instead of $W(F)$, so they can be determined exactly by measuring $\Delta(F)$.

method to approximate the integral by extending its limit to $\theta_i = \pm\infty$ (Carrier et al., 2005). Further, by using the Fourier transform of the Dirac delta function δ (Carrier et al., 2005):

$$\delta(g) = \frac{1}{2\pi}\int_{-\infty}^{+\infty} \exp(Ikg)dk, \tag{26}$$

where I is the imaginary identity that satisfies $I^2 = -1$, we can rewrite the partition function Eq. 25 as:

$$Z = \frac{1}{2\pi}\int_{-\infty}^{+\infty}\cdots\int_{-\infty}^{+\infty} \exp\left[-\beta(E - Fx) + Ikg\right]\ d\vec{\theta}\, dk. \tag{27}$$

Consider the exponent in the partition function Eq. 27: the Hamiltonian $\beta(E - Fx)$ is quadratic in θ_i and independent of k (see Eq. 4) and the constraint function g is linear in θ_i (see Eq. 24). So the whole exponent $[-\beta(E - Fx) + Ikg]$ is quadratic in θ_i and k and therefore we can write it in a matrix form[4] $-\vec{\Theta}^T\mathbf{M}\vec{\Theta}$ (excluding a constant term βFL, which can be taken out of the integral), where $\vec{\Theta} = [\theta_1, \theta_2, \cdots \theta_N, k]^T$. Then the partition function Eq. 27 can be evaluated analytically:

$$\begin{aligned} Z &= \frac{e^{\beta FL}}{2\pi}\int_{-\infty}^{+\infty} \exp\left[-\left(\vec{\Theta}^T\mathbf{M}\vec{\Theta}\right)\right] d\vec{\Theta} &(28)\\ &= \frac{e^{\beta FL}}{2\pi}\sqrt{\frac{\pi^{N+1}}{\det\mathbf{M}}}. &(29)\end{aligned}$$

The $(N+1)$ dimensional matrix $\mathbf{M}$, whose upper $N \times N$ submatrix is a tridiagonal matrix, can be written compactly as[5]:

$$[\mathbf{M}]_{ij} = \begin{cases} \beta(\kappa_{i-1} + \kappa_i + f)\delta_{ij} - \beta\kappa_t \cdot \delta_{(|i-j|,1)} & 1 \le i, j \le N \\ -[1 - \delta_{i,(N+1)}\delta_{j,(N+1)}] \cdot I/2 & \text{otherwise} \end{cases} \tag{30}$$

where $t = \min(i, j)$ and δ is the Kronecker delta. A similar mathematical technique for evaluating the partition function has been applied for circular DNA by Zhang and Crothers (2003).

Eq. 29 is the analytic expression for the partition function that involves a determinant $\det\mathbf{M}$. We calculate this determinant in Appendix A and the result is:

$$\det\mathbf{M} = \frac{N\beta^{N-1}}{4} \times \prod_{i=1}^{N-1}\lambda_i, \tag{31}$$

where λ_i is a sequence that contains information about the bending modulus sequence κ_i:

$$\lambda_1 = 2\kappa_1 + f, \quad \lambda_i = (2\kappa_i + f) - \frac{\kappa_i\kappa_{i-1}}{\lambda_{i-1}} \quad (i = 2, 3, \cdots N-1). \tag{32}$$

[4]One of the three steps in the Laplace method is to expand the exponent around its minimum point (Carrier et al., 2005), so it is proper to use the Taylor expansion expressions Eq. 4 and Eq. 24.

[5]Here to make the expression compact, we introduce $\kappa_0 = \kappa_N = 0$

Plugging the expression for $\det \mathbf{M}$ (Eq. 31) into the partition function (Eq. 29), we get:

$$\log Z = -\frac{N-1}{2}\log\beta + FL\beta - \frac{1}{2}\log\left(\frac{N\prod_{i=1}^{N-1}\lambda_i}{\pi^{N-1}}\right). \tag{33}$$

Comparing Eq.33 with Eq. 10 and noticing that the number of degrees of freedom is $D = (N-1)$ because we have one position constraint on the end of the chain, we get the analytic expression for $W(F)$:

$$W(F) = \frac{1}{2}\left[\sum_{i=1}^{N-1}\log\lambda_i + \log\left(\frac{N}{\pi^{N-1}}\right)\right]. \tag{34}$$

Therefore,

$$\Delta(F) = \frac{dW(F)}{dF} = \frac{1}{2}\sum_{i=1}^{N-1}\frac{\lambda_i'}{\lambda_i}, \tag{35}$$

where $\lambda_i' = d\lambda_i/dF$.

By substituting Eq. 34 and Eq. 35 into Eq. 12 through Eq. 21, we get all the thermo-mechanical quantities for the 2D heterogeneous hinged-hinged chain. In particular, the force-extension relation is:

$$\langle x\rangle = L - k_BT\cdot\Delta(F) = L - \frac{k_BT}{2}\cdot\sum_{i=1}^{N-1}\frac{\lambda_i'}{\lambda_i}. \tag{36}$$

To verify our result, we apply Eq. 36 to a homogeneous chain and compare it with the known theory for the homogeneous hinged-hinged continuous rod. We consider the limit as the segment length $l \to 0$ while the contour length $L = Nl$ is held fixed so that the discrete chain becomes a continuous rod. We show in Appendix B that in this special limit case, Eq. 36 exactly reduces to the well-known force-extension relation for a homogeneous fluctuating rod (Purohit et al., 2008):

$$\langle x_{\text{homo}}\rangle = L - \frac{Lk_BT}{4\sqrt{KF}}\coth\left(\frac{FL}{\sqrt{KF}}\right) + \frac{k_BT}{4F}. \tag{37}$$

Another special case is a continuous rod with 2 separated regions of bending modulus K_I and K_{II} respectively. This special heterogeneous rod is suitable for studying the forced-unfolding of proteins because the bending moduli of folded and unfolded proteins are expected to be different. Let L_I and L_{II} be the contour length of the 2 homogeneous sub-rods ($L_I + L_{II} = L$). We show in Appendix C that the extension of such a rod is given by:

$$\langle x\rangle = L - \frac{k_BT}{2}\left[\frac{\frac{1}{E_1\sqrt{F}}\cosh\left(\sqrt{\frac{F}{F_1}}\right) + \frac{2\overline{K^{-1/2}}}{F}\sinh\left(\sqrt{\frac{F}{F_1}}\right) + \frac{1}{E_0\sqrt{F}}\cosh\left(\sqrt{\frac{F}{F_0}}\right) + \frac{\Delta K^{-1/2}}{F}\sinh\left(\sqrt{\frac{F}{F_0}}\right)}{4\overline{K^{-1/2}}\sinh\left(\sqrt{\frac{F}{F_1}}\right) + 2\Delta K^{-1/2}\sinh\left(\sqrt{\frac{F}{F_0}}\right)} - \frac{1}{F}\right], \tag{38}$$

where

$$\overline{K^{-1/2}} = \frac{1}{2}\left(\frac{1}{\sqrt{K_I}} + \frac{1}{\sqrt{K_{II}}}\right), \quad \Delta K^{-1/2} = \frac{1}{\sqrt{K_I}} - \frac{1}{\sqrt{K_{II}}}, \tag{39}$$

$$E_1 = \left(\frac{L}{\sqrt{K_I K_{II}}} + \frac{L_I}{K_I} + \frac{L_{II}}{K_{II}}\right)^{-1}, \quad E_0 = \left(\frac{L}{\sqrt{K_I K_{II}}} - \frac{L_I}{K_I} - \frac{L_{II}}{K_{II}}\right)^{-1}, \tag{40}$$

$$F_1 = \left(\frac{L_{II}}{\sqrt{K_{II}}} + \frac{L_I}{\sqrt{K_I}}\right)^{-2}, \quad F_0 = \left(\frac{L_{II}}{\sqrt{K_{II}}} - \frac{L_I}{\sqrt{K_I}}\right)^{-2}. \tag{41}$$

Note that in general, the extension of the rod is not the sum of the extensions of the two homogeneous sub-rods (Eq. 37) because (1) the two sub-rods do not necessarily satisfy the hinged-hinged boundary conditions so Eq. 37 is not applicable to either of them; (2) there is bending cooperativity at the interface of the two sub-rods.

3.3. Partially clamped 2D chain

For the partially clamped conditions, one end of the chain is still fixed at the origin but the other end is free to have transverse displacement instead of being constrained on the $\hat{X}$ axis (Fig. 1(b)). However, moments are applied such that both angles at the two ends are zero:

$$\theta_1 = \theta_N = 0. \tag{42}$$

With the conditions in Eq. 42, the Hamiltonian (Eq. 4) can be rewritten in terms of only $(N-2)$ angles from θ_2 to θ_{N-1}:

$$\beta(E - Fx) = \sum_{i=2}^{N-1} \beta(\kappa_{i-1} + \kappa_i + f)\theta_i^2 - 2\sum_{i=2}^{N-2} \beta\kappa_i\theta_i\theta_{i+1} - \beta FL. \tag{43}$$

The partition function for a partially clamped chain is:

$$Z = \int_{-\infty}^{+\infty} \cdots \int_{-\infty}^{+\infty} \exp\left[-\beta(E - Fx)\right] d\vec{\theta}, \tag{44}$$

where $d\vec{\theta} = [\, d\theta_2 \cdots d\theta_{N-1} \,]$.

We plug in the Hamiltonian (Eq. 43) into Eq. 44 and again write the exponent in Eq. 44 in matrix form $-(\vec{\theta}^T \mathbf{M} \vec{\theta})$ (excluding a constant term βFL, which can be written outside the integral), so that the partition function now becomes:

$$Z = e^{\beta FL} \int_{-\infty}^{+\infty} \exp\left[-\vec{\theta}^T \mathbf{M} \vec{\theta}\right] d\vec{\theta} = e^{\beta FL} \sqrt{\frac{\pi^{N-2}}{\det \mathbf{M}}}, \tag{45}$$

where in this case, $\mathbf{M}$ is a $(N-2)$ dimensional tridiagonal matrix and it can be written compactly as:

$$[\mathbf{M}]_{ij} = \beta\left(\kappa_i + \kappa_{i+1} + f\right)\delta_{ij} - \beta\kappa_{t+1}\delta_{|i-j|,1}, \tag{46}$$

with $t = \min(i, j)$.

By performing elementary row operations on $\mathbf{M}$ and evaluating its eigenvalues, we find that its determinant is given by:

$$\det \mathbf{M} = \beta^{N-2} \times \prod_{i=1}^{N-2} \lambda_i, \tag{47}$$

where the sequence λ_i, different from the one in the hinged-hinged case, is given by:

$$\lambda_1 = \kappa_1 + \kappa_2 + f, \quad \lambda_i = (\kappa_i + \kappa_{i+1} + f) - \frac{\kappa_i^2}{\lambda_{i-1}} \quad (i = 2, 3, \cdots N-2). \tag{48}$$

By substituting Eq. 47 into Eq. 45 and comparing the expression of $\log Z$ with Eq. 10, we obtain the analytic expression for $W(F)$ and $\Delta(F)$:

$$W(F) = \frac{1}{2}\left[\sum_{i=1}^{N-2} \log \lambda_i - (N-2)\log \pi\right], \tag{49}$$

$$\Delta(F) = \frac{1}{2}\sum_{i=1}^{N-2} \frac{\lambda_i'}{\lambda_i}, \tag{50}$$

where again $\lambda_i' = d\lambda_i/dF$.

Suprisingly, $\Delta(F)$ has the same form as in the hinged-hinged case. But, we emphasize that the sequence λ_i here is different from the one in the hinged-hinged case (Eq. 32 and Eq. 48).

Again, by substituting Eq. 49 and Eq. 50 into Eq. 12 through Eq. 21, we obtain all the thermo-mechanical quantities.

3.4. Clamped-clamped 2D chain

For the clamped-clamped chain, the two tangent angles at the ends are constrained to zero and the ends of the chain are constrained on the $\hat{X}$ axis (Fig. 1(c)). The Hamiltonian is the same as the one in the partially clamped case given in Eq. 43.

The position constraint function, Eq. 24, which states that the end of the chain must lie on the $\hat{X}$ axis, can also be expressed in terms of the $(N-2)$ angles $\theta_2, \theta_3, \cdots \theta_{N-1}$:

$$g \approx \sum_{i=2}^{N-1} \theta_i = 0. \tag{51}$$

The partition function for a clamped-clamped chain is:

$$\begin{aligned} Z &= \int_{-\infty}^{+\infty} \cdots \int_{-\infty}^{+\infty} \exp\left[-\beta(E - Fx)\right] \delta(g)\, d\vec{\theta} & (52)\\ &= \frac{1}{2\pi}\int_{-\infty}^{+\infty} \cdots \int_{-\infty}^{+\infty} \exp\left[-\beta(E - Fx) + Ikg\right] d\vec{\theta}\, dk, & (53) \end{aligned}$$

where Eq. 26 has been used and $d\vec{\theta} = [\, d\theta_2 \cdots d\theta_{N-1}\,]$.

Again, to evaluate the partition function, we plug Eq. 43 and Eq. 51 into Eq. 53 and express the exponent in a quadratic form $-\vec{\Theta}^T\mathbf{M}\vec{\Theta}$ (excluding a constant term βFL, which can be written outside the integral), where $\vec{\Theta} = [\theta_2, \cdots \theta_{N-1}, k]^T$, then the partition function can be evaluated analytically as:

$$Z = \frac{e^{\beta FL}}{2\pi}\sqrt{\frac{\pi^{N-1}}{\det \mathbf{M}}}, \tag{54}$$

where the $(N-1)$ dimensional matrix $\mathbf{M}$ in this case is:

$$[\mathbf{M}]_{ij} = \begin{cases} \beta\left(\kappa_i + \kappa_{i+1} + f\right)\delta_{ij} - \beta\kappa_{t+1}\delta_{|i-j|,1} & 1 \le i,j \le N-2 \\ -I(1-\delta_{i,(N-1)}\delta_{j,(N-1)})/2 & \text{otherwise} \end{cases} \tag{55}$$

again, $t = \min(i,j)$.

We show in Appendix D that in this case, the determinant $\det \mathbf{M}$ is:

$$\det \mathbf{M} = \left(\frac{\beta^{N-3}R}{4}\right)\prod_{i=1}^{N-2}\lambda_i, \tag{56}$$

with the sequence of λ_i being the same as the one in the partially clamped case given in Eq. 48 and the quantity R is given by:

$$R = \sum_{i=1}^{N-2}(\kappa_i + \kappa_{i+1} + f)g_i^2 - 2\sum_{i=1}^{N-3}\kappa_{i+1}g_i g_{i+1}, \tag{57}$$

with

$$g_{N-2} = \frac{\rho_{N-2}}{\lambda_{N-2}},\ g_i = \frac{\rho_i + \kappa_{i+1}g_{i+1}}{\lambda_i}\,(i = N-3, N-2, \cdots 1),\ \rho_i = 1 + \sum_{j=1}^{i-1}\left(\prod_{s=i-j+1}^{i}\frac{\kappa_s}{\lambda_{s-1}}\right). \tag{58}$$

We plug Eq. 56 into Eq. 54, compare the expression for $\log Z$ with Eq. 10 to find the expressions for $W(F)$ and $\Delta(F)$ (note that the number of degrees of freedom in this case is $D = N-3$):

$$W(F) = \frac{1}{2}\left[\sum_{i=1}^{N-2}\log\lambda_i + \log R - (N-3)\log\pi\right], \tag{59}$$

$$\Delta(F) = \frac{1}{2}\left[\sum_{i=1}^{N-2}\frac{\lambda_i'}{\lambda_i} + \frac{R'}{R}\right], \tag{60}$$

where $R' = dR/dF$.

With Eq. 59 and Eq. 60, all the thermo-mechanical quantities can be computed. In particular, the force-extension relation for a clamped-clamped chain is:

$$\langle x\rangle = L - k_BT\cdot\Delta(F) = L - \frac{k_BT}{2}\left[\sum_{i=1}^{N-2}\frac{\lambda_i'}{\lambda_i} + \frac{R'}{R}\right]. \tag{61}$$

3.5. Fluctuation of a 2D chain

In addition to the thermo-mechanical quantities discussed above, we are also interested in the quantity $\langle \theta_i \cdot \theta_j \rangle$, because it reflects how much the chain is fluctuating. Also, by calculating $\langle \theta_i \cdot \theta_j \rangle$, we immediately get the fluctuation of the chain in the Y direction, which has been measured in experiments for some biopolymers (Arsenault et al., 2007):

$$\langle y_i^2 \rangle = \left\langle \left(\sum_{j=1}^{i} l \sin\theta_j \right) \left(\sum_{k=1}^{i} l \sin\theta_k \right) \right\rangle \approx l^2 \sum_{j,k=1}^{i} \langle \theta_j \cdot \theta_k \rangle, \tag{62}$$

where y_i is the transverse displacement of the i-th segment in the Y direction (Fig. 1).

The quantity $\langle \theta_i \cdot \theta_j \rangle$ by definition is:

$$\langle \theta_i \cdot \theta_j \rangle = \frac{1}{Z} \sum_{\nu} (\theta_i \cdot \theta_j) \exp[-\beta(E_\nu - F x_\nu)]. \tag{63}$$

By writing it in integral form, we can evaluate it using the following formula (Reichl, 1980; Zhang and Crothers, 2003):

$$\begin{aligned} \langle \theta_i \cdot \theta_j \rangle &= \frac{\int_{-\infty}^{+\infty} (\theta_i \cdot \theta_j) \exp[-\vec{\Theta}^T \mathbf{M} \vec{\Theta}] \, d\vec{\Theta}}{\int_{-\infty}^{+\infty} \exp[-\vec{\Theta}^T \mathbf{M} \vec{\Theta}] \, d\vec{\Theta}} & (64) \\ &= \frac{1}{2} \left(\mathbf{M}^{-1} \right)_{ij}, & (65) \end{aligned}$$

where the detailed expressions and dimensionality of $\mathbf{M}$ and $\vec{\Theta}$ depend on the boundary conditions as has been discussed in the previous sections (Eq. 30, Eq. 46 and Eq. 55). For the analytic formula of the inverse of a tridiagonal matrix, we refer the reader to da Fonseca and Petronilho (2001).

Note that for the partially clamped chain, from Eq. 46, we know that:

$$\langle \theta_i \cdot \theta_j \rangle = \frac{1}{2} \left(\mathbf{M}^{-1} \right)_{ij} \sim \beta^{-1} \sim T, \tag{66}$$

and therefore using Eq. 62, we conclude that the transverse fluctuation of the chain scales linearly with respect to T:

$$\langle y_i^2 \rangle \sim T. \tag{67}$$

Recall that the variance in the extension x scales as T^2 (Eq. 16). So as temperature T increases, the fluctuation in x should be more significant compared to the transverse fluctuation.

We show in Appendix E that Eq. 66 also holds for the hinged-hinged chain and the clamped-clamped chain. So the conclusion that the transverse fluctuation scales as T holds for all the boundary conditions discussed in this paper.

3.6. Theory for the 3D chains

We will show in this section that by choosing a suitable set of angles that represents the configuration of the chain, the results for a 2D chain can be easily generalized to a 3D one.

Let $\hat{X}$, $\hat{Y}$ and $\hat{Z}$ be the standard reference triad in 3D space. As before, a force $\vec{F} = F\hat{X}$ is acting on one end of the chain while the other end is fixed at the origin. We denote the unit tangent vector of the 3D chain as $\hat{t}(s)$, which forms an angle $\theta(s)$ with respect to the $\hat{X}$ axis. The projection of $\hat{t}$ on the $\hat{Y}$-$\hat{Z}$ plane forms an angle ϕ with respect to the $\hat{Y}$ axis so that $\hat{t}(s)$ can be written as:

$$\hat{t} = [\cos\theta, \sin\theta\cos\phi, \sin\theta\sin\phi]. \tag{68}$$

It follows then:

$$\left|\frac{d\hat{t}}{ds}\right|^2 = \dot{\theta}^2 + \sin^2\theta\dot{\phi}^2, \tag{69}$$

where $\dot{\theta}$ and $\dot{\phi}$ are the derivative of θ and ϕ with respect to the arc length s.

We will discuss the 3D hinged-hinged chain below in detail. 3D chains under the other two boundary conditions can be studied following the same procedure, though some detailed steps are different, the final results turn out be the same and we will give a summary in the end of this section.

We define:

$$\vartheta_x = \theta\cos\phi, \quad \vartheta_y = \theta\sin\phi, \tag{70}$$

so that:

$$\vartheta_x^2 + \vartheta_y^2 = \theta^2, \quad \dot{\vartheta_x}^2 + \dot{\vartheta_y}^2 = \dot{\theta}^2 + \theta^2\dot{\phi}^2. \tag{71}$$

Representation of the 3D chains using ϑ_x and ϑ_y has been discussed in Kulić (2004).

The Hamiltonian of the 3D chain, up to a quadratic approximation, can be written as [6]:

$$\begin{aligned}
\mathscr{H}_{3D} &= \beta(E - Fx) = \int_0^L \frac{\beta K}{2}\left|\frac{d\hat{t}}{ds}\right|^2 ds - \beta F\int_0^L \cos\theta ds & (72)\\
&\approx \int_0^L \frac{\beta K}{2}\left(\dot{\theta}^2 + \theta^2\dot{\phi}^2\right) ds - \beta F\int_0^L \left(1 - \frac{\theta^2}{2}\right) ds & (73)\\
&= \left[\int_0^L \frac{\beta K}{2}\dot{\vartheta_x}^2 ds - \beta F\int_0^L \left(1 - \frac{\vartheta_x^2}{2}\right) ds\right] + \left[\int_0^L \frac{\beta K}{2}\dot{\vartheta_y}^2 ds - \beta F\int_0^L \left(1 - \frac{\vartheta_y^2}{2}\right) ds\right] + \beta FL & (74)
\end{aligned}$$

Here Eq. 69 and Eq. 71 have been used. Comparing Eq. 74 with Eq. 3, we conclude that:

$$\mathscr{H}_{3D} = \mathscr{H}_{2D}(\vartheta_x) + \mathscr{H}_{2D}(\vartheta_y) + \beta FL, \tag{75}$$

where $\mathscr{H}_{2D}(\vartheta)$ represents the Hamiltonian of the 2D chain with tangent angle denoted as ϑ.

[6] We assume that there are no torsional constraints here. Problems with torsional or other constraints can be addressed using the same method as long as the Hamiltonian can be expressed as a quadratic form. Also, see Nelson (2008) for explanations when the twisting energy can be neglected.

There are two constraints for the 3D chain: the Y and Z coordinates of the end of the chain should be zero. They relate to the constraint function in the 2D problem in the following ways (see Eq. 24 for the 2D constraint function):

$$g_Y = \int_0^L \sin\theta\cos\phi\, ds \approx \int_0^L \vartheta_x ds = g_{2D}(\vartheta_x), \tag{76}$$

$$g_Z = \int_0^L \sin\theta\sin\phi\, ds \approx \int_0^L \vartheta_y ds = g_{2D}(\vartheta_y). \tag{77}$$

Note that the two constraint functions are decoupled in terms of the angles ϑ_x and ϑ_y up to a linear approximation, which is sufficient for using the Laplace method to evaluate the partition function, as we have shown in the 2D case.

Hence, using Eq. 75, Eq. 76 as well as Eq. 77, the partition function for a 3D chain is:

$$Z_{3D} = \int_{-\infty}^{+\infty}\int_{-\infty}^{+\infty} \exp\left(-\mathscr{H}_{3D}\right)\delta(g_Y)\delta(g_Z) d\vec{\vartheta}_x d\vec{\vartheta}_y \tag{78}$$

$$= e^{-\beta FL}\int_{-\infty}^{+\infty} \exp\left[-\mathscr{H}_{2D}(\vartheta_x)\right]\delta\left[g_{2D}(\vartheta_x)\right] d\vec{\vartheta}_x \cdot \int_{-\infty}^{+\infty} \exp\left[-\mathscr{H}_{2D}(\vartheta_y)\right]\delta\left[g_{2D}(\vartheta_y)\right] d\vec{\vartheta}_y \tag{79}$$

$$= e^{-\beta FL}(Z_{2D})^2. \tag{80}$$

Eq. 80 relates the 3D partition function with the 2D partition function, from which we further get:

$$\log Z_{3D} = -\beta FL + 2\log Z_{2D} = -\beta FL + 2\left[-\frac{D_{2D}}{2}\log\beta + FL\beta - W_{2D}(F)\right] \tag{81}$$

$$= -\frac{D_{3D}}{2}\log\beta + \beta FL - 2W_{2D}(F), \tag{82}$$

where Eq. 10 has been used. Here the number of degrees of freedom of a 3D chain is twice of that of a 2D chain ($D_{3D} = 2D_{2D}$) because for each segment, we have θ_i and also ϕ_i. Comparing Eq. 82 with Eq. 10, we get:

$$W_{3D}(F) = 2W_{2D}(F), \tag{83}$$

and therefore:

$$\Delta_{3D}(F) = 2\cdot\Delta_{2D}(F), \quad \Delta'_{3D}(F) = 2\cdot\Delta'_{2D}(F). \tag{84}$$

With the relations of 2D and 3D $\Delta(F)$, we conclude using Eq. 12 through Eq. 19 that for a 3D chain, the following quantities are twice of those of the 2D chain: the entropy S, the shrinking of the chain $L - \langle x\rangle$, average energy $\langle E\rangle$, the heat capacity C_F and the variances of the extension and the energy $\langle(\Delta x)^2\rangle$, $\langle(\Delta E)^2\rangle$.

To relate the fluctuation of a 3D chain with a 2D one, note that the transverse displacement of the 3D chain is:

$$\langle\, y(s)_{3D}^2 + z(s)_{3D}^2\,\rangle = \left\langle\left(\int_0^s \sin\theta\cos\phi\, ds\right)^2 + \left(\int_0^s \sin\theta\sin\phi\, ds\right)^2\right\rangle \tag{85}$$

$$\approx \left\langle\left(\int_0^s \vartheta_x ds\right)^2 + \left(\int_0^s \vartheta_y ds\right)^2\right\rangle \tag{86}$$

$$= 2\langle\, y(s)_{2D}^2\,\rangle. \tag{87}$$

So the transverse fluctuation is twice larger for the 3D chain.

Finally, we note that for the partially clamped and clamped-clamped 3D chain, the corresponding boundary conditions are that for the first and last segment of the chain:

$$\theta = \vartheta_x = \vartheta_y = 0 \tag{88}$$

The derivations are almost the same as the hinged-hinged chain and are not shown here. The results of Eq. 83, Eq. 84 as well as Eq. 87 remain the same as for the hinged-hinged chain.

4. Monte Carlo Simulation

To verify our theory, we have done Monte Carlo (MC) simulations for the 2D fluctuating chains under an external applied force for all the three boundary conditions. The chain is represented by the N tangent angles θ_i as in the theoretical model and it is initially straight.

At each MC step, a new conformation is generated from the existing one by randomly varying N of the θ_i. Each valid change of the configuration should satisfy the boundary conditions. A new conformation is accepted with a probability according to the Metropolis criterion (Allen and Tildesley, 1987) and the thermo-mechanical quantities and fluctuations of the chain are recorded. To check if equilibrium has been reached in a given simulation, we ensure that the equipartition theorem (Eq. 8) is satisfied. Results are recorded only at equilibrium.

5. Results and Application

5.1. thermo-mechanical properties of the chain

Fig. 3 shows the thermo-mechanical quantities for a homogeneous fluctuating 500-segment chain under different boundary conditions. The contour length of the chain is $L = 2.5$nm and the bending modulus is $K = 2.5k_BT\cdot$nm so that $\xi_p/L = 2$ (2D), where ξ_p is the persistence length of the chain. Several interesting results are shown in this figure: (1) All the results show that the hinged-hinged chain is the most flexible. It has the smallest extension under an applied force and it has the largest variances in extension and energy. On the other hand, the clamped-clamped chain is the least flexible, which is expected because it has the smallest number of degrees of freedom. (2) The variances of extension and energy are decreasing functions of the applied force F. In other words, force suppresses the fluctuations of the chain. (3) Coefficient of thermal expansion α is negative and it is increasing with F. (4) The hinged-hinged chain and partially clamped chain have similar results for the thermo-mechanical quantities that are determined only by $\Delta(F)$ and $\Delta'(F)$, but not $W(F)$. This can be understood by comparing the expressions of $\Delta(F)$ for these two boundary conditions (Eq. 35 and Eq. 50).

Eq. 23, which relates the response of the chain to the force and to temperature, is verified in MC simulations. Average extension and thermal expansion coefficient are recorded in simulations under forces varying from 150pN to 1150pN. The result is shown in Fig. 4.

The force-extension relation for a homogeneous continuous rod has been studied under all the three boundary conditions (Purohit et al., 2008). To check our results, we plot the

force extension relation for a homogeneous chain and compare it with the known theory for the rod in Fig. 5. Here we choose a large $N = 50000$ so that $l = L/N << L$ and the chain is approximately a smooth rod. Fig. 5 shows that our formulae for all the boundary conditions reduce to the known theory for the homogeneous rods when N is large and l is small.

The computational complexity using the formulae for thermo-mechanical properties shown in this paper is $O(N)$. This is true not only for homogeneous chains, but for any heterogeneous chain under all the three boundary conditions. Note that we need at least N values of K_i to specify an arbitrary heterogeneous chain, so $O(N)$ is the optimal computational complexity for the problem.

5.2. Fluctuation and correlation of the angle θ_i

Fig. 6 shows the fluctuation in θ_i (i.e., $\langle\theta_i^2\rangle$) along the chain. The profile depends strongly on the boundary conditions when $\xi_p/L > 1$ (Fig. 6(a) shows the case when $\xi_p/L = 5$). In this case, the hinged-hinged chain has maximum fluctuation at the two ends whereas the partially clamped and clamped-clamped chains have minimum fluctuations there, which is expected because $\theta_1 = \theta_N \equiv 0$ for these two chains. In the middle point of the chain, the hinged-hinged chain and the partially clamped chain achieve their smallest and largest fluctuations respectively. It is interesting that the maximum fluctuation for the clamped-clamped chain does not occur in the middle of the chain (Fig. 6(a) black). When ξ_p/L becomes small, the boundary conditions only influence the profile near the two ends of the chain (Fig. 6(b)). Away from the two ends, the profiles almost coincide for different boundary conditions.

Fig. 7 shows the dependence of the $\langle\theta_i^2\rangle$ profile on the heterogeneity of the chain. The theoretical predictions are compared to the MC simulation results for all the three boundary conditions. For all the cases studied here, a jump in the bending modulus leads to a corresponding jump in the $\langle\theta_i^2\rangle$ profile. The larger the bending modulus, the smaller the value of $\langle\theta_i^2\rangle$. The figures imply that the heterogeneity of the chain has a significant influence on $\langle\theta_i^2\rangle$.

Fig. 8 shows the correlation in the θ angles. In particular, we show $\langle\theta(s)\cdot\theta(L/2)\rangle$ here. Clearly, the profiles should have a peak at $s = L/2$ and decrease as s moves away from $L/2$. The smaller the persistence length ξ_p is compared to the contour length L, the faster the profile decreases. Again, the results show that the profiles depend strongly on the boundary conditions when $\xi_p/L \approx 1$. For the partially clamped chain, our theory predicts that the correlation decreases but remains positive along the chain whereas for the hinged-hinged and clamped-clamped chains, the correlations can become negative near the two ends of the chain, although for the clamped-clamped chain, due to the constraints that $\theta_1 = \theta_N \equiv 0$, the correlation is exactly 0 at the ends. The MC simulation results confirm our predictions. In order to show the theoretical prediction clearly, we plot the simulation results separately in (b), (d) and (f). In addition, we show in Fig. 8(g) (theory) and (h) (MC simulation) that the correlation profile is not symmetric for a heterogeneous chain. The correlation decreases faster where the bending modulus is smaller.

5.3. Transverse fluctuation of the chains $\langle y^2\rangle$

Fig. 9(a) shows the transverse fluctuation of the chain in the Y direction. As shown in the figure, the transverse fluctuation depends on the boundary conditions and the heterogeneity of the chain. For chains with the same bending modulus, the partially clamped chain has the

largest transverse fluctuation while the clamped-clamped chain has the smallest fluctuation, which is expected because the clamped-clamped chain has the smallest number of degrees of freedom. Fig. 9(b) shows that the fluctuation decreases when the force increases. The theoretical predictions and the MC simulation results match quite well.

Fig. 10(a)-(c) show that for a fixed persistence length, the chain that has longer contour length has more transverse fluctuation. Our theoretical predictions and the MC simulation results match quite well for all the three boundary conditions.

5.4. Application to the protein unfolding problem

The mechanical behavior of proteins is studied in experiments by stretching oligomers in an atomic force microscope. As the protein chain is stretched, the number of unfolded oligomers increases in steps and this gives rise to a characteristic saw-tooth pattern in the force-extension profile as seen in Fig. 11 (experimental data from Chyan et al. (2004)). The loss of structural integrity in the unfolded regions is expected to change the stiffness of the chain. We can study these effects through our heterogeneous fluctuating chain model. To see how this can be achieved we refer the reader to the force-extension curves in Fig. 11. The blue dotted curves in Fig. 11 are the experimental data of forced unfolding of a chain of ubiquitins under constant velocity pulling from Chyan et al. (2004). Each peak in the profile represents an unfolding event where the force drops precipitously. There are six experimental curves in Fig. 11 (see the descriptions in Chyan et al. (2004)) and the last curve corresponds to the force-extension relation of a chain of purely unfolded ubiquitins. We model the entire protein oligomer as a fluctuating chain with two bending moduli K_f (for folded proteins) and K_u (for unfolded proteins), each part with length $N_f L_{fs}$ and $N_u L_{us}$, where N_f, N_u are the number of folded and unfolded proteins (they are changing from curve to curve) and L_{fs}, L_{us} are the contour lengths of a single folded and unfolded protein respectively. We first fit the last curve, which corresponds to six unfolded ubiquitins, with the homogeneous model (Eq. 37) and obtain two parameters K_u and L_{us} for the unfolded protein. Similarly, we fit the first curve to obtain the other two parameters K_f and L_{fs} for the folded protein (Fig. 11(a), red circles are the fitted data and black curves are the fitting results). Then without any more free parameters, we apply the force-extension relation for a 'special heterogeneous chain' (Eq. 38, 3D version) to predict all the intermediate curves using different values of N_f and N_u (Fig. 11(b), red curves). As shown in Fig. 11(b), our prediction matches the experimental data quite well.

6. Conclusion

In this paper we have developed a method to determine the thermo-mechanics of heterogeneous fluctuating elastic rods and chains with arbitrary boundary conditions. In particular, we are able to compute the force-extension relation and the variance of transverse fluctuation of the chain. Our results are in excellent agreement with Monte Carlo simulations. We have demonstrated the usefulness of our method by using it to interpret experimental data on the stretching of proteins. Our method assumes that there are no torsional constraints on the rod. But, problems with torsional or other constraints can be addressed using this method as long as the energy can be expressed as a quadratic form in the kinematic variables. The framework developed in this paper is not restricted to one-dimensional rods or chains alone.

In fact, our goal is to extend this technique to two- and three-dimensional problems, such as, those involving the mechanics of networks of filaments.

Appendix

A. det M for the hinged-hinged chain

The $(N+1)$ dimension matrix $\mathbf{M}$ for the hinged-hinged case is given by (Eq. 30), which is:

$$\mathbf{M} = \begin{pmatrix} \beta(\kappa_1+f) & -\beta\kappa_1 & 0 & \cdots & 0 & -I/2 \\ -\beta\kappa_1 & \beta(\kappa_1+\kappa_2+f) & -\beta\kappa_2 & \cdots & 0 & -I/2 \\ 0 & -\beta\kappa_2 & \beta(\kappa_2+\kappa_3+f) & \cdots & 0 & -I/2 \\ & \cdots & \cdots & \cdots & \cdots & \\ 0 & 0 & 0 & \cdots & -\beta\kappa_{N-1} & -I/2 \\ 0 & 0 & 0 & \cdots & \beta(\kappa_{N-1}+f) & -I/2 \\ -I/2 & -I/2 & -I/2 & \cdots & -I/2 & 0 \end{pmatrix} \tag{89}$$

To evaluate the determinant of $\mathbf{M}$, we introduce another matrix $\mathbf{M}^*$ as:

$$\mathbf{M}^* = \mathbf{R}^T\mathbf{P}\mathbf{M}\mathbf{Q}\mathbf{R}, \tag{90}$$

where the (N+1) dimensional matrices $\mathbf{R}$, $\mathbf{P}$ and $\mathbf{Q}$ are:

$$\mathbf{P} = \mathrm{diag}\left(\beta^{-1}, \beta^{-1}, \cdots, \beta^{-1}, 2I\right), \tag{91}$$

$$\mathbf{Q} = \mathrm{diag}\left(1, 1, \cdots, 1, 2I\beta\right), \tag{92}$$

$$\mathbf{R} = \begin{pmatrix} 1 & 0 & 0 & \cdots & 0 & 0 & 0 \\ 1 & 1 & 0 & \cdots & 0 & 0 & 0 \\ 1 & 1 & 1 & \cdots & 0 & 0 & 0 \\ & \cdots & \cdots & \cdots & \cdots & & \\ 1 & 1 & 1 & \cdots & 1 & 0 & 0 \\ 1 & 1 & 1 & \cdots & 1 & 1 & 0 \\ 0 & 0 & 0 & \cdots & 0 & 0 & 1 \end{pmatrix} \tag{93}$$

From Eq. 90 and the definitions of the matrics $\mathbf{P}$, $\mathbf{Q}$ and $\mathbf{R}$, we get:

$$\det\mathbf{M} = -\frac{\beta^{N-1}}{4}\det\mathbf{M}^*. \tag{94}$$

Now we need to evaluate $\det\mathbf{M}^*$.

Using Eq. 90, we get the matrix $\mathbf{M}^*$:

$$\mathbf{M}^* = \begin{pmatrix} \mathbf{M}_{\mathrm{in}} & \vec{G} \\ \vec{G}^T & 0 \end{pmatrix}, \tag{95}$$

where the N dimensional $\mathbf{M}_{\rm in}$ is given by:

$$\mathbf{M}_{\rm in} = \begin{pmatrix} Nf & (N-1)f & (N-2)f & \cdots & 2f & f \\ (N-1)f & \kappa_1+(N-1)f & (N-2)f & \cdots & 2f & f \\ (N-2)f & (N-2)f & \kappa_2+(N-2)f & \cdots & 2f & f \\ & \cdots & \cdots & \cdots & \cdots & \\ 2f & 2f & 2f & \cdots & \kappa_{N-2}+2f & f \\ f & f & f & \cdots & f & \kappa_{N-1}+f \end{pmatrix} \tag{96}$$

and N dimensional vector $\vec{G}^T$ is given by:

$$\vec{G}^T = [N, N-1, N-2, \cdots, 2, 1]\,. \tag{97}$$

But for the type of matrix in form of Eq. 95, we have the following formula (see Zhang and Crothers (2003)):

$$\det \mathbf{M}^* = -\det \mathbf{M}_{\rm in} \left(\vec{G}^T \cdot \mathbf{M}_{\rm in}^{-1} \vec{G}\right). \tag{98}$$

So now we need to compute $\det \mathbf{M}_{\rm in}$ as well as $\vec{G}^T \cdot \mathbf{M}_{\rm in}^{-1}\vec{G}$.

We first perform elementary row operations on $\mathbf{M}_{\rm in}$, transform it into a diagonal matrix and find its determinant given by:

$$\det \mathbf{M}_{\rm in} = f \prod_{i=1}^{N-1} \lambda_i, \tag{99}$$

where the sequence λ_i is given by:

$$\lambda_1 = 2\kappa_1 + f, \quad \lambda_i = (2\kappa_i + f) - \frac{\kappa_i \kappa_{i-1}}{\lambda_{i-1}} \quad (i = 2, 3, \cdots N-1). \tag{100}$$

Next, to evaluate $\vec{G}^T \cdot \mathbf{M}_{\rm in}^{-1}\vec{G}$, we define $\vec{g}$ as:

$$\mathbf{M}_{\rm in}\, \vec{g} = \vec{G}, \tag{101}$$

so that

$$\vec{G}^T \cdot \mathbf{M}_{\rm in}^{-1}\vec{G} = \vec{g}^T \cdot \mathbf{M}_{\rm in}\, \vec{g}, \tag{102}$$

where the symmetry property of $\mathbf{M}_{\rm in}$ has been used. But Eq. 101 is easy to solve and one can verify that:

$$\vec{g}^T = \left[f^{-1}, 0, 0, \cdots, 0, 0\right], \tag{103}$$

and therefore using Eq. 96, Eq. 102 and Eq. 103, we get:

$$\vec{G}^T \mathbf{M}_{\rm in}^{-1}\vec{G} = \frac{N}{f}. \tag{104}$$

Finally, Eq.94, Eq. 98, Eq. 99 together with Eq. 104 leads to:

$$\det \mathbf{M} = \frac{N\beta^{N-1}}{4} \times \prod_{i=1}^{N-1} \lambda_i. \tag{105}$$

B. Force-extension relation for a homogeneous wormlike chain

For a homogeneous chain, we have $K_i \equiv K$ and $\kappa_i \equiv \kappa$. Using the definition of the sequence λ_i for a hinged-hinged chain (Eq. 32), one can verify by mathematical induction that:

$$\prod_{k=i}^{N-1} \lambda_k = \lambda_i \cdot p_{N-i-1} - rd \cdot p_{N-i-2}, \quad (i \leq N-2) \tag{106}$$

where r, d are given by:

$$r = \frac{2\kappa + f + \sqrt{4\kappa f + f^2}}{2}, \quad d = \frac{2\kappa + f - \sqrt{4\kappa f + f^2}}{2}, \tag{107}$$

and the sequence p_i is given by:

$$p_i = \frac{r^{i+1} - d^{i+1}}{r - d}. \tag{108}$$

Using Eq. 106 to Eq. 108 and also Eq. 32, we get:

$$\prod_{k=1}^{N-1} \lambda_k \;\; = \;\; \lambda_1 \cdot p_{N-2} - rd \cdot p_{N-3} = \frac{r^N - d^N}{r - d}. \tag{109}$$

Hence,

$$\sum_{k=1}^{N-1} \frac{\lambda_i'}{\lambda_i} \;\; = \;\; \frac{d}{dF}\left(\log \prod_{k=1}^{N-1} \lambda_k\right) \tag{110}$$

$$= \;\; \frac{Nr'}{r} \cdot \frac{1 - \left(\frac{d}{r}\right)' \cdot \left(\frac{d}{r}\right)^{N-1}}{1 - \left(\frac{d}{r}\right)^N} - \frac{r'}{r} \cdot \frac{1 - \left(\frac{d}{r}\right)'}{1 - \left(\frac{d}{r}\right)}. \tag{111}$$

Using the definitions of r, d (Eq. 107) as well as those for κ, f (Eq. 5), we get:

$$r = \frac{K}{2L}N + \frac{\sqrt{KF}}{2} + O(N^{-1}), \tag{112}$$

$$r' = \frac{1}{4}\sqrt{\frac{K}{F}} + \frac{L}{4N} + O(N^{-2}), \tag{113}$$

$$d = \frac{K}{2L}N - \frac{\sqrt{KF}}{2} + O(N^{-1}), \tag{114}$$

$$d' = -\frac{1}{4}\sqrt{\frac{K}{F}} + \frac{L}{4N} + O(N^{-2}). \tag{115}$$

Plugging Eq. 112 to Eq. 115 into Eq. 111, taking the limit as $N \to +\infty$, we get:

$$\lim_{N\to\infty} \sum_{k=1}^{N-1} \frac{\lambda_i'}{\lambda_i} \;\; = \;\; \frac{1}{2}\left[\frac{L}{\sqrt{KF}} \coth\left(L\sqrt{\frac{F}{K}}\right) - \frac{1}{F}\right]. \tag{116}$$

Putting Eq. 116 into Eq. 36, we recover the force-extension relation for a homogeneous hinged-hinged continuous rod (Purohit et al., 2008):

$$\langle x_{\text{homo}} \rangle = L - \frac{Lk_BT}{4\sqrt{KF}} \coth\left(\frac{FL}{\sqrt{KF}}\right) + \frac{k_BT}{4F}. \tag{117}$$

C. Force-extension relation for a special heterogeneous wormlike chain

For a special heterogeneous wormlike chain, we have

$$\kappa_i = \begin{cases} \kappa_I & 1 \le i \le s \\ \kappa_{II} & (s+1) \le i \le N \end{cases} \tag{118}$$

Here s is an integer indicating the segment that separates the two regions of the chain (s is not the arc length in this section).

Hence, under hinged-hinged conditions, the sequence λ_i is (Eq. 32):

$$\lambda_i = \begin{cases} 2\kappa_I + f & i = 1 \\ 2\kappa_I + f - \frac{\kappa_I^2}{\lambda_{i-1}} & 2 \le i \le s \\ 2\kappa_{II} + f - \frac{\kappa_I \kappa_{II}}{\lambda_s} & i = s+1 \\ 2\kappa_{II} + f - \frac{\kappa_{II}^2}{\lambda_{i-1}} & s+2 \le i \le (N-1) \end{cases} \tag{119}$$

Using mathematical induction, one can verify that:

$$\prod_{k=i}^{N-1} \lambda_k = \begin{cases} p_{N-i-1}\lambda_i - r_2 d_2 \cdot p_{N-i-2} & (s+1) \le i \le (N-2) \\ p_{N-s-1}\lambda_s - \kappa_I \kappa_{II} \cdot p_{N-s-2} & i = s \\ p_{N-i-1}\lambda_i - r_1 d_1 \cdot p_{N-i-2} & 1 \le i \le (s-1) \end{cases} \tag{120}$$

where p_i, r_i and d_i are given by:

$$p_i = \begin{cases} \frac{r_2^{i+1} - d_2^{i+1}}{r_2 - d_2} & 0 \le i \le (N-s-2) \\ (r_2 + d_2)p_{N-s-2} - r_2 d_2 p_{N-s-3} & i = N-s-1 \\ \frac{r_1^{i-N+s+2} - d_1^{i-N+s+2}}{r_1 - d_1} \cdot p_{N-s-1} - \frac{r_1^{i-N+s+1} - d_1^{i-N+s+1}}{r_1 - d_1} \cdot \kappa_I \kappa_{II} \cdot p_{N-s-2} & N-s \le i \le (N-2) \end{cases} \tag{121}$$

$$r_1 = \frac{2\kappa_I + f + \sqrt{4\kappa_I f + f^2}}{2}, \quad d_1 = \frac{2\kappa_I + f - \sqrt{4\kappa_I f + f^2}}{2}, \tag{122}$$

$$r_2 = \frac{2\kappa_{II} + f + \sqrt{4\kappa_{II} f + f^2}}{2}, \quad d_2 = \frac{2\kappa_{II} + f - \sqrt{4\kappa_{II} f + f^2}}{2}. \tag{123}$$

In particular, using Eq. 120 and setting $i = 1$, we get:

$$\prod_{k=1}^{N-1} \lambda_k = \frac{\left(r_2^{N-s} - d_2^{N-s}\right)\left(r_1^{s+1} - d_1^{s+1}\right) - \kappa_I \kappa_{II}\left(r_2^{N-s-1} - d_2^{N-s-1}\right)\left(r_1^s - d_1^s\right)}{(r_1 - d_1)(r_2 - d_2)}. \tag{124}$$

Note that Eq. 124 reduces to the homogeneous case (Eq. 109) when we set $s = 0$, or $s = N-1$, or $r_1 = r_2$, $d_1 = d_2$.

Using Eq. 122, Eq. 123 as well as Eq. 5, we have:

$$\frac{r_i'}{r_i} = \frac{L}{2K_i}\sqrt{\frac{K_i}{F}}\frac{1}{N} + O(N^{-3}), \tag{125}$$

$$\frac{d_i}{r_i} = 1 - \frac{2L\sqrt{K_i F}}{K_i N} + \frac{2FL^2}{K_i N^2} + O(N^{-3}), \tag{126}$$

$$\left(\frac{d_i}{r_i}\right)^u = \exp(\frac{-2uL\sqrt{K_i F}}{NK_i}) + O(N^{-2}) \tag{127}$$

where u is a function of N and it satisfies $u(N) \sim N$ as $N \to +\infty$.

$$\frac{d_i'}{r_i'} = -1 + 2L\sqrt{\frac{F}{K_i}}\frac{1}{N} + O(N^{-2}), \tag{128}$$

$$\frac{\kappa_i}{r_i} = 1 - \frac{L\sqrt{K_i F}}{K_i N} + O(N^{-2}). \tag{129}$$

Here to make the formulae compact, we use κ_1, κ_2, K_1, K_2 to denote κ_I, κ_{II}, K_I and K_{II}. Note that the subscripts 1 and 2 in this section do not mean the 1st and 2nd segments of the chain.

Similarly as in Appendix B, we can use Eq. 125 to Eq. 129 to evalute $\sum \lambda_i'/\lambda_i$ and then the function $\Delta(F)$ (take $N \to +\infty$ while keeping $Nl = L$ fixed), the result is:

$$\Delta(F) = \frac{\frac{1}{E_1\sqrt{F}}\cosh\left(\sqrt{\frac{F}{F_1}}\right) + \frac{2\overline{K^{-1/2}}}{F}\sinh\left(\sqrt{\frac{F}{F_1}}\right) + \frac{1}{E_0\sqrt{F}}\cosh\left(\sqrt{\frac{F}{F_0}}\right) + \frac{\Delta K^{-1/2}}{F}\sinh\left(\sqrt{\frac{F}{F_0}}\right)}{8\overline{K^{-1/2}}\sinh\left(\sqrt{\frac{F}{F_1}}\right) + 4\Delta K^{-1/2}\sinh\left(\sqrt{\frac{F}{F_0}}\right)} - \frac{1}{2F}. \tag{130}$$

The meanings of $\overline{K^{-1/2}}$, $\Delta K^{-1/2}$, E_1, E_0, F_1 and F_0 are given in Eq. 39 to Eq. 41. Using $x = L - k_B T\Delta(F)$ (Eq. 13), we get the force-extension relation for a special heterogeneous rod, which is shown in the main text (Eq. 38).

D. det M for the clamped-clamped chain

The $(N-1)$ dimensional matrix $\mathbf{M}$ for the clamped-clamped chain is given by Eq. 55, which is:

$$\mathbf{M} = \begin{pmatrix} \beta(\kappa_1+\kappa_2+f) & -\beta\kappa_2 & 0 & \cdots & 0 & -I/2 \\ -\beta\kappa_2 & \beta(\kappa_2+\kappa_3+f) & -\beta\kappa_3 & \cdots & 0 & -I/2 \\ 0 & -\beta\kappa_3 & \beta(\kappa_3+\kappa_4+f) & \cdots & 0 & -I/2 \\ & \cdots & \cdots & \cdots & \cdots & \\ 0 & 0 & 0 & \cdots & -\beta\kappa_{N-2} & -I/2 \\ 0 & 0 & 0 & \cdots & \beta(\kappa_{N-2}+\kappa_{N-1}+f) & -I/2 \\ -I/2 & -I/2 & -I/2 & \cdots & -I/2 & 0 \end{pmatrix} \tag{131}$$

To evaluate the determinant of $\mathbf{M}$, we introduce another matrix $\mathbf{M}^*$ as:

$$\mathbf{M}^* = \mathbf{PMQ}, \tag{132}$$

where the $(N-1)$ dimensional matrix $\mathbf{P}$ and $\mathbf{Q}$ are:

$$\mathbf{P} = \mathrm{diag}\left(\beta^{-1}, \beta^{-1}, \cdots, \beta^{-1}, 2I\right), \tag{133}$$

$$\mathbf{Q} = \mathrm{diag}\left(1, 1, \cdots, 1, 2I\beta\right). \tag{134}$$

Note that the matrics $\mathbf{P}$ and $\mathbf{Q}$ defined here are the same as those defined for the hinged-hinged chain (Eq. 91 and Eq. 92) except that their dimensionalities are different.

From Eq. 132 and the definitions of the matrics $\mathbf{P}$, $\mathbf{Q}$, we get:

$$\det \mathbf{M} = -\frac{\beta^{N-3}}{4} \det \mathbf{M}^*. \tag{135}$$

Now we need to evaluate $\det \mathbf{M}^*$.

Using Eq. 132, we get the matrix $\mathbf{M}^*$:

$$\mathbf{M}^* = \begin{pmatrix} \mathbf{M}_{\mathrm{in}} & \vec{G} \\ \vec{G}^T & 0 \end{pmatrix}, \tag{136}$$

where the $(N-2)$ dimensional $\mathbf{M}_{\mathrm{in}}$ in this case is given by:

$$\mathbf{M}_{\mathrm{in}} = \begin{pmatrix} \kappa_1+\kappa_2+f & -\kappa_2 & 0 & \cdots & 0 \\ -\kappa_2 & \kappa_2+\kappa_3+f & -\kappa_3 & \cdots & 0 \\ 0 & -\kappa_3 & \kappa_3+\kappa_4+f & \cdots & 0 \\ & \cdots & \cdots & \cdots & \\ 0 & 0 & 0 & \cdots & -\kappa_{N-2} \\ 0 & 0 & 0 & \cdots & \kappa_{N-2}+\kappa_{N-1}+f \end{pmatrix} \tag{137}$$

and $(N-2)$ dimensional vector $\vec{G}^T$ is given by:

$$\vec{G}^T = [1, 1, 1, \cdots, 1, 1]. \tag{138}$$

Again, for the type of matrix in form of Eq. 136, we have the formula (Zhang and Crothers, 2003):

$$\det \mathbf{M}^* = -\det \mathbf{M}_{\mathrm{in}} \left(\vec{G}^T \cdot \mathbf{M}_{\mathrm{in}}^{-1} \vec{G}\right). \tag{139}$$

So now we need to compute $\det \mathbf{M}_{\mathrm{in}}$ as well as $\vec{G}^T \cdot \mathbf{M}_{\mathrm{in}}^{-1} \vec{G}$.

We first perform the elementary row operations on $\mathbf{M}_{\mathrm{in}}$ and find that its determinant is given by:

$$\det \mathbf{M}_{\mathrm{in}} = \prod_{i=1}^{N-2} \lambda_i, \tag{140}$$

where the sequence λ_i is given by:

$$\lambda_1 = \kappa_1 + \kappa_2 + f, \quad \lambda_i = (\kappa_i + \kappa_{i+1} + f) - \frac{\kappa_i^2}{\lambda_{i-1}} \quad (i = 2, 3, \cdots N-2). \tag{141}$$

Next, to evaluate $\vec{G}^T \cdot \mathbf{M}_{\text{in}}^{-1}\vec{G}$, which we will denote as R below, we again define $\vec{g}$ as:

$$\mathbf{M}_{\text{in}}\,\vec{g} = \vec{G}, \tag{142}$$

so that

$$R = \vec{G}^T \cdot \mathbf{M}_{\text{in}}^{-1}\vec{G} = \vec{g}^T \cdot \mathbf{M}_{\text{in}}\,\vec{g}. \tag{143}$$

We solve Eq. 142 and get $\vec{g}$:

$$g_{N-2} = \frac{\rho_{N-2}}{\lambda_{N-2}}, \quad g_i = \frac{\rho_i + \kappa_{i+1}g_{i+1}}{\lambda_i}. \quad (i = N-3, N-4, \cdots 1) \tag{144}$$

where the sequence ρ_i is given by:

$$\rho_i = 1 + \sum_{j=1}^{i-1}\left(\prod_{s=i-j+1}^{i}\frac{\kappa_s}{\lambda_{s-1}}\right). \tag{145}$$

Therefore using Eq. 137, Eq. 143 and Eq. 144, we get:

$$R = \sum_{i=1}^{N-2}(\kappa_i + \kappa_{i+1} + f)g_i^2 - 2\sum_{i=1}^{N-3}\kappa_{i+1}g_i g_{i+1}. \tag{146}$$

Finally, Eq.135, Eq. 139, Eq. 140, Eq. 143 together with Eq. 146 lead to:

$$\det\mathbf{M} = \left(\frac{\beta^{N-3}R}{4}\right)\prod_{i=1}^{N-2}\lambda_i. \tag{147}$$

E. Transverse fluctuation scales as T

We need to show $\langle y_i^2\rangle \sim T$ for the hinged-hinged and clamped-clamped chain in this section. For chains under both the boundary conditions, the matrix $\mathbf{M}$ have the form (see Eq. 89 and Eq. 131):

$$\mathbf{M} = \begin{pmatrix} \beta\mathbf{J} & \vec{v} \\ \vec{v}^T & 0 \end{pmatrix}. \tag{148}$$

Using Eq. 148, one can verify by matrix multiplication (or see Zhang and Crothers (2003)) that:

$$\mathbf{M}^{-1} = \begin{pmatrix} \beta^{-1}\left[\mathbf{J}^{-1} - \mathbf{J}^{-1}\vec{v}\left(\vec{v}^T\mathbf{J}^{-1}\vec{v}\right)^{-1}\vec{v}^T\mathbf{J}^{-1}\right] & \mathbf{J}^{-1}\vec{v}\left(\vec{v}^T\mathbf{J}^{-1}\vec{v}\right)^{-1} \\ \left(\vec{v}^T\mathbf{J}^{-1}\vec{v}\right)^{-1}\vec{v}^T\mathbf{J}^{-1} & -\beta\left(\vec{v}^T\mathbf{J}^{-1}\vec{v}\right)^{-1} \end{pmatrix}. \tag{149}$$

Note that $\langle\theta_i\cdot\theta_j\rangle$ is determined by the upper corner submatrix of $\mathbf{M}^{-1}$ (Eq. 65, the rest of the elements in the matrix $\mathbf{M}^{-1}$ correspond to $\langle\theta_i\cdot k\rangle$, which we are not interested in. Here k is from the Fourier transform of the Dirac delta function in Eq. 26). Therefore, noticing that both $\mathbf{J}$ and $\vec{v}$ do not depend on β, we have:

$$\langle\theta_i\cdot\theta_j\rangle = \left(\mathbf{M}^{-1}\right)_{ij} = \beta^{-1}\left[\mathbf{J}^{-1} - \mathbf{J}^{-1}\vec{v}\left(\vec{v}^T\mathbf{J}^{-1}\vec{v}\right)^{-1}\vec{v}^T\mathbf{J}^{-1}\right]_{ij} \sim T. \tag{150}$$

Finally, using the relation between $\langle y_i^2\rangle$ and $\langle\theta_i\cdot\theta_j\rangle$ (Eq. 62), we conclude that:

$$\langle y_i^2\rangle \sim T. \tag{151}$$

References

Ahsan, A., Rudnick, J., Bruinsma, R., 1998. Elasticity theory of the B-DNA to S-DNA transition. Biophys. J. 74(1), 132-137.

Allen, M.P., Tildesley, D.J., 1987. Computer Simulation of Liquids. Oxford Science, Oxford.

Arsenault, M.E., Zhao, H., Purohit, P.K., Goldman, Y.E., Bau, H.H., 2007. Confinement and manipulation of actin filaments by electric fields. Biophys. J. 93(8):L42-L44.

Bustamante, C., Marko, J.F., Siggia, E.D., Smith, S., 1994. Entropic elasticity of lambda-phage DNA. Science 265(5178), 1599-1600.

Callen, H.B., 1985. Thermodynamics and an Introduction to Thermostatistics, second ed. John Wiley and Sons, New York, Chichester, Brisbane, Toronto, Singapore.

Carrier, G.F., Krook, M., Pearson, C.E., 2005. Functions of a Complex Variable: Theory and Technique, Society for Industrial and Applied Mathematics, Philadelphia, PA.

Chyan, C.L., Lin, F.C., Peng. H., Yuan, J.M., Chang, C.H., Lin, S.H., Yang, G., 2004. Reversible mechanical unfolding of single ubiquitin molecules. Biophys. J. 87(6):3995-4006.

da Fonseca, C.M., Petronilho, J., 2001. Explicit inverse of some tridiagonal matrices. Linear Algebra Appl. 325:7-21.

Geissler, P.L., Shakhnovich, E.I., 2002. Reversible stretching of random heteropolymers. Phys. Rev. E 65(5 Pt 2), 056110.

Hagerman, P.J., 1988. Flexibility of DNA. Annu. Rev. Biophys. Biophys. Chem. 17, 265-286.

Hogan, M., Legrange, J., Austin, B., 1983. Dependence of DNA helix flexibility on base composition. Nature 304(5928), 752-754.

Jarkova, E., Vlugt, T.J., Lee, N.K., 2005. Stretching a heteropolymer. J. Chem. Phys. 122(11), 114904.

Kulić, I., 2004. Statistical Mechanics of Protein Complexed and Condensed DNA. Thesis, Max Planck Institute for Polymer Research, Mainz, Germany.

Marko, J.F., Siggia, E.D., 1995. Stretching DNA. Macromolecules 28(26), 8759-8770.

Moukhtar, J., Fontaine, E., Faivre-Moskalenko, C., Arneodo, A., 2007. Probing persistence in DNA curvature properties with atomic force microscopy. Phys. Rev. Lett. 98(17), 178101.

Nelson, P., 2008. Biological Physics: Energy, Information, Life, updated first ed. W. H. Freeman and Company, New York.

Odijk, T., 1995. Stiff chains and filaments under tension. Macromolecules 28(20), 7016-7018.

Popov, Y.O., Tkachenko, A.V., 2007. Effects of sequence disorder on DNA looping and cyclization. Phys. Rev. E 76(2 Pt 1), 021901.

Purohit, P.K., Arsenault, M.E., Goldman, Y., Bau, H.H., 2008. The mechanics of short rod-like molecules in tension. Int. J. Non-linear Mech. 43(10):1056-1063.

Purohit, P.K., Nelson, P.C., 2006. Effect of supercoiling on formation of protein-mediated DNA loops. Phys. Rev. E 74(6 Pt 1), 061907.

Reichl, L.E., 1998. A Modern Course in Statistical Physics, second ed. Wiley-Interscience, New York.

Seol, Y., Li, J., Nelson, P.C., Perkins, T.T., Betterton, M.D., 2007. Elasticity of short DNA molecules: theory and experiment for contour lengths of 0.6-7 microm. Biophys. J. 93(12), 4360-4373.

Su, T., Purohit, P.K., 2009. Mechanics of forced unfolding of proteins. Acta Biomater. 5(6):1855-1863.

Wilson, D.P., Lillian, T., Goyal, S., Tkachenko, A.V., Perkins, N.C., Meiners, J., 2007. Understanding the role of thermal fluctuations in DNA looping. Proceeding of the SPIE. 6602, 660208.

Zhang, Y., Crothers, D.M., 2003. Statistical mechanics of sequence-dependent circular DNA and its application for DNA cyclization. Biophys. J. 84(1), 136-153.

Captions

Figure 1

Model of the 2D chain. A thermally fluctuating $N-$segment 2D chain is subjected to an external applied force $\vec{F} = F\hat{X}$. The configuration of the chain is characterized by its N tangent angles θ_i, formed by the segments with respect to the $\hat{X}$ axis. The transverse displacement of the chain, denoted by y_i in the figure, reflects how much the chain fluctuates. (a) Hinged-hinged boundary conditions: both ends of the chain are constrained on the $\hat{X}$ axis, but no moment is acting on them; (b) partially clamped boundary conditions: one end of the chain is clamped on the $\hat{X}$ aixs while the other end, with slope also constrained to be zero, is free to have transverse displacement in the Y direction. (c) clamped-clamped boundary conditions: both ends are clamped on the $\hat{X}$ axis.

Figure 2

The unkown function $W(F)$ can be measured in a single force extension experiment. The shaded area above the force-extension curve is the complementary energy and the area beneath the force-extension curve is $k_BT \cdot W(F)$ by Eq. 15.

Figure 3

Thermo-mechanical quantities for a fluctuating chain. Blue: hinged-hinged boundary conditions; red: partially clamped boundary conditions; black: clamped-clamped boundary conditions. (a) Force-extension profile of the chain. Inset: local profile shows that the hinged-hinged chain (blue) has smaller extension and thus is more flexible (to show the figure clearly, we have changed the circles into lines with the same colors); (b) Variance of the extension. Inset: local profile shows that the hinged-hinged chain (blue) fluctuates more than the partially clamped chain (to show the figure clearly, we have changed the circles into lines with the same colors); (C) Average energy of the chain versus the applied force; (D) Variance of the energy; (E) Thermal expansion coefficient α versus the applied force; (F) Isothermal extensibility χ versus the applied force.

Figure 4

Verifying Eq. 23. Solid line: theoretical prediciton; circles: MC simulation results. Simulations have been done under 11 different forces varying from 150pN to 1150pN with an increasement of 100pN. Temperature is set to be 300K. Relative extension as well as thermal expansion coefficient are recorded. The result shown is for a homogeneous chain with contour length $L = 25$nm and bending modulus $K = 2.5k_BT \cdot nm$.

Figure 5

Force-extension relation for homogeneous chains (blue curve) and rods (red circle, theory in Purohit et al. (2008)). (a) Hinged-hinged boundary conditions; (b) partially clamped boundary conditions; (c) clamped-clamped boundary conditions. $K = 2.5k_BT \cdot nm$, $L =$ 2.5nm. The figures show that our force-extension relations for the chains reduce to the known formulae for the continuous rods when $N \to +\infty$ with $L = Nl$ fixed. Here $N = 50000$ for the blue curves.

Figure 6

Dependence of the fluctuation of θ angles on the boundary conditions. Blue: hinged-hinged chain, the fluctuation in θ is at maximum and minimum respectively at the two ends and in the middle of the chain; red: partially clamped chain, the fluctuation is at maximum and minimum respectively in the middle and at the two ends; black: clamped-clamped chain, the fluctuation is at minimum at the two ends, but the maximum is not achieved in the middle of the chain. Also, the partially clamped chain (red) fluctuates more than the clamped-clamped chain (black). (a) $\xi_p/L = 5$, the dependence on the boundary conditions is significant througout the chain; (b) $\xi_p/L = 0.2$ the dependence on the boundary conditions is significant only at the two ends of the chain. To make the figures clear, the MC simulation results are not shown in the same figures.

Figure 7

Dependence of the fluctuation of θ angles on the heterogeneity of the chain. Blue: homogeneous chain with $K = 2.5k_BT \cdot nm$; black: corresponding MC simulation results; red: heterogeneous chain with two bending moduli: $K_I = 0.5k_BT \cdot nm$ at the first half of the chain and $K_{II} = 4.5k_BT \cdot nm$ at the second half; black dashed curve: corresponding MC simulation results. (a), (b) and (c) are for hinged-hinged, partially clamped and clamped-clamped boundary conditions respectively. The figures show that jumps in the bending modulus result in jumps in the fluctuation in the $\langle\theta^2\rangle$ profile. The larger the bending modulus, the smaller the fluctuation in θ.

Figure 8

Correlation in the tangent angle θ. (a-f): results for the homogeneous chains. Blue: $\xi_p/L = 5$; red: $\xi_p/L = 1$; black: $\xi_p/L = 0.2$. (a),(c),(e) are the theoretical results for the hinged-hinged, partially clamped and clamped-clamped chains respectively. To make the plots clear, we plot the corresponding MC simulation results separately in (b),(d) and (f) (circles). The figures show that the correlation in θ depends strongly on ξ_p/L. When $\xi_p/L > 1$ (blue), the profile also significantly depends on the boundary conditions. (g-h): results for a heterogeneous chain with $L = 1$nm. The first half and the second half of the chain have bending moduli of $K_I = 0.5k_BT \cdot nm$ and $K_{II} = 4.5k_BT \cdot nm$ respectively. (g) is the theoretical predictions and (h) is the MC simulation results. Blue, red and black colors are for the hinged-hinged, partially clamped and clamped-clamped boundary conditions respectively. The correlation profile loses its symmetry and decreases faster at the first half of the chain where the bending modulus is smaller.

Figure 9

Transverse fluctuation $\langle y^2\rangle$. (a): blue: hinged-hinged chain; red: partially clamped chain; black: clamped-clamped chain. Solid curve: homogeneous chain with $K = 2.5k_BT \cdot nm$; dashed curve: heterogeneous chain with $K_I = 0.5k_BT \cdot nm$ for the first half of the chain and $K_{II} = 4.5k_BT \cdot nm$ for the second half. In (a), $L = 1nm$ for all the curves. Since the curves are close to each other, to make the theoretical results clear, we do not plot the MC simulation results in (a). (b): transverse fluctuation decreases when the force increases. The results are for a homogeneous hinged-hinged chain with $L = 25$nm and $K = 2.5k_BT \cdot nm$. The corresponding forces are labeled in the figure. Circles: MC simulation results; solid lines: theoretical predictions.

Figure 10

Dependence of the transverse fluctuation on the countour length of the chain. $K = 2.5k_BT \cdot nm$ for all the curves. Black solid curves (theory) and blue circles (MC simulation): $L = 5$nm; black dashed curves (theory) and red circles (MC simulation): $L = 25$nm; (a) hinged-hinged boundary conditions; (b) partially clamped boundary conditions; (c) clamped-clamped boundary conditions. The figures show that for a fixed persistence length, the longer the chain, the more the fluctuation. Also, our theoretical results and the MC simulation results match quite well. Note that here $\xi_p/L \leq 1$ and the results for hinged-hinged chain and clamped-clamped chains are quite similar, which is confirmed by the simulation results.

Figure 11

Unfolding of six copies of ubiquitins under constant velocity pulling condition. Blue dotted curves are the experimental data from Chyan et al. (2004). Each peak in the profile represents a unfolding event where the force drops. The first and the last experimental curves are fitted to obtain the contour lengths and the bending moduli of the folded and unfolded proteins (Fig.(a): red circles are the fitted data and the black curves are the fitting results). The intermediate curves are then predicted without any free parameters using the 3D version of Eq. 38 (Fig.(b), red curves). Figure.(b) shows that the predictions match well with the experimental data.

Figures

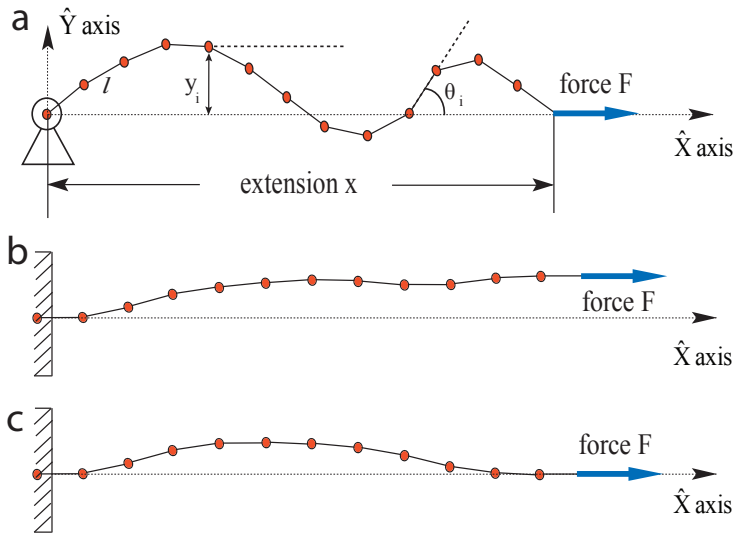

Figure 1:

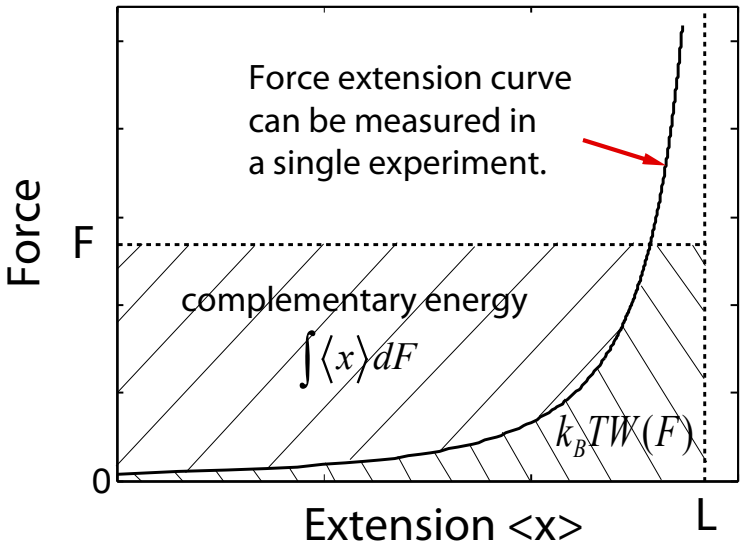

Figure 2:

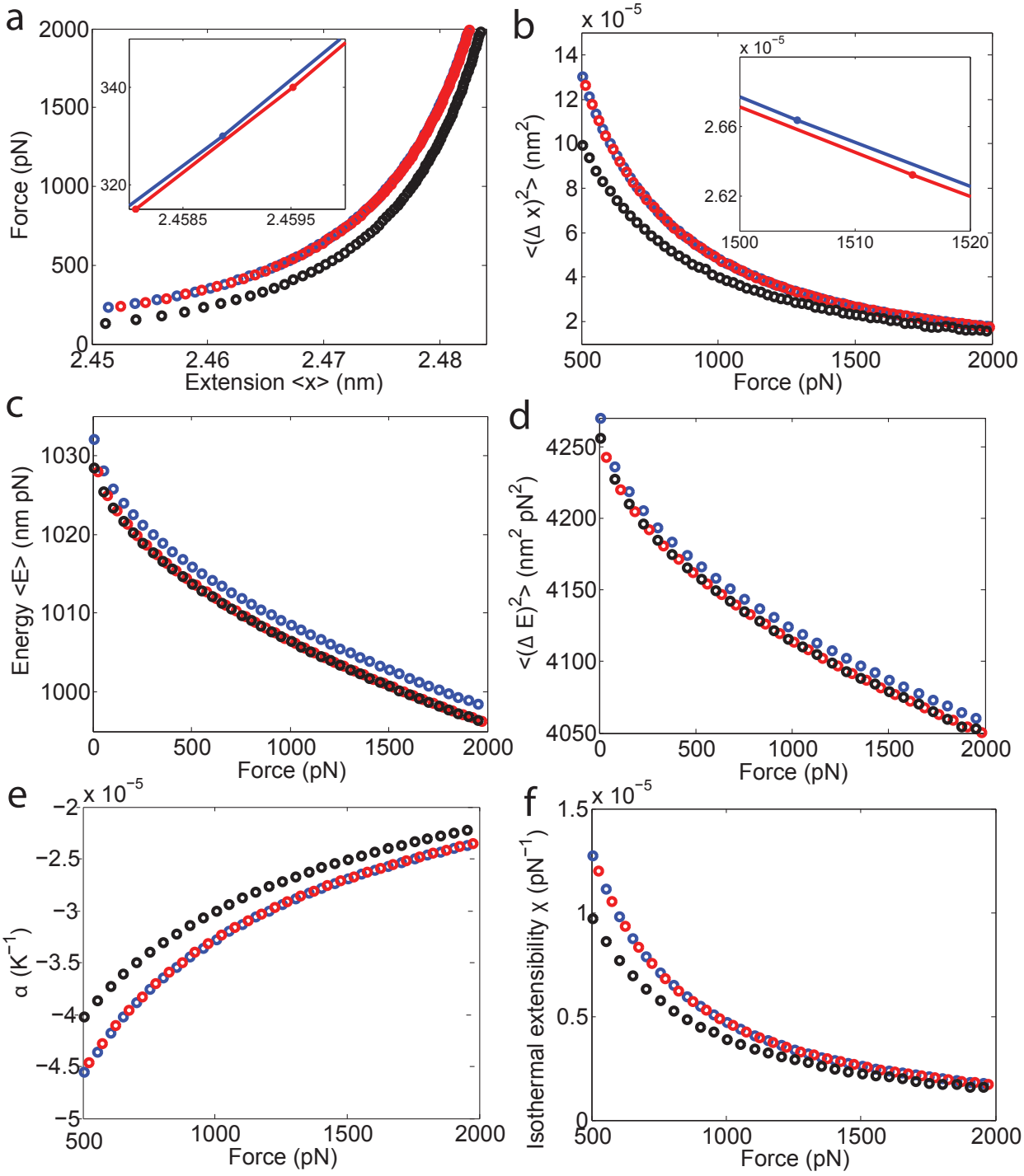
a
Force (pN)
Extension <x> (nm)
b
x 10^-5
<(Δ x)^2> (nm^2)
Force (pN)
c
Energy <E> (nm pN)
Force (pN)
d
<(Δ E)^2> (nm^2 pN^2)
Force (pN)
e
x 10^-5
α (K^-1)
Force (pN)
f
x 10^-5
Isothermal extensibility χ (pN^-1)
Force (pN)

Figure 3:

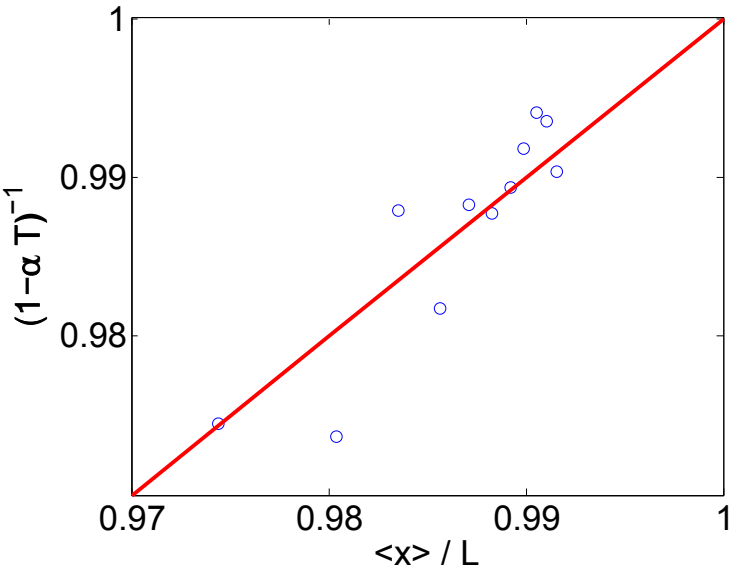

Figure 4:

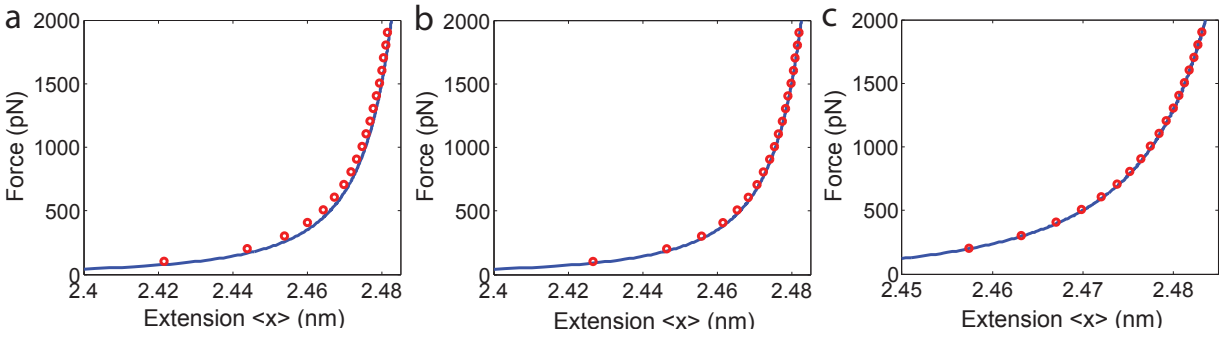

Figure 5:

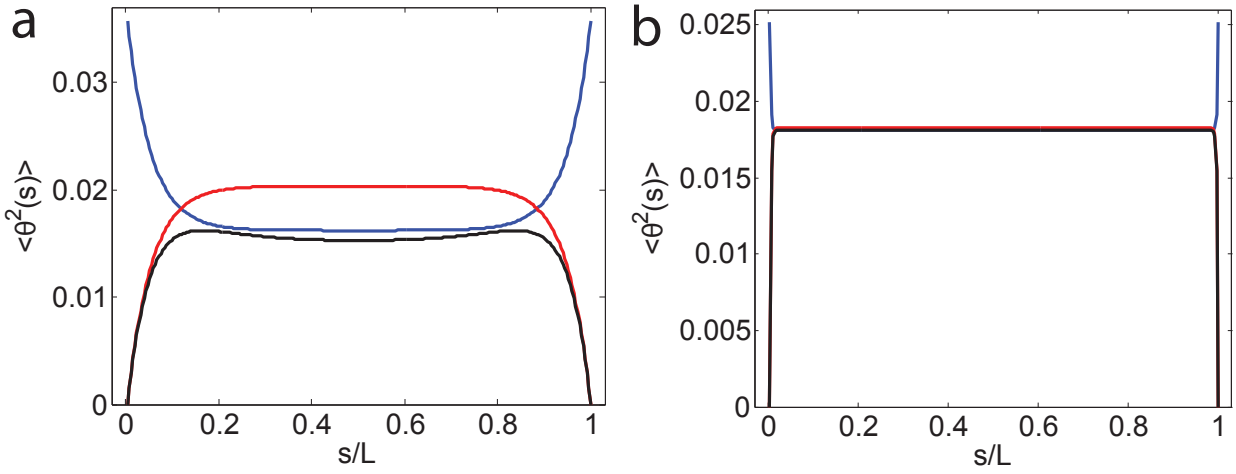

Figure 6:

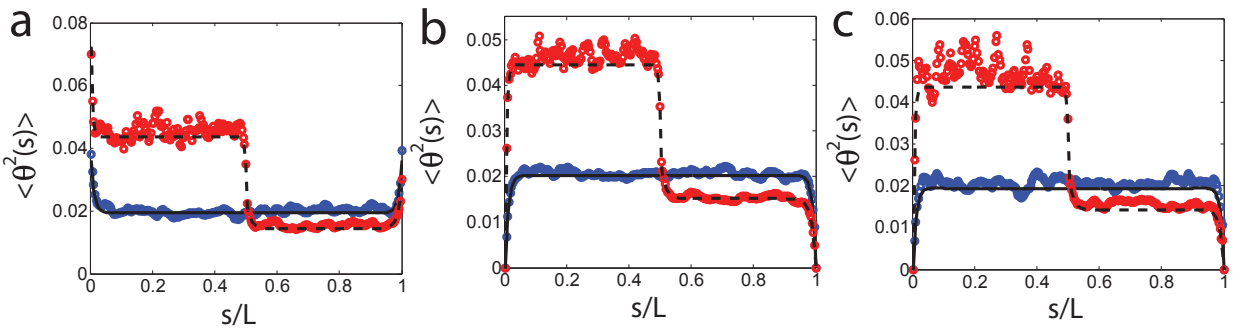

Figure 7:

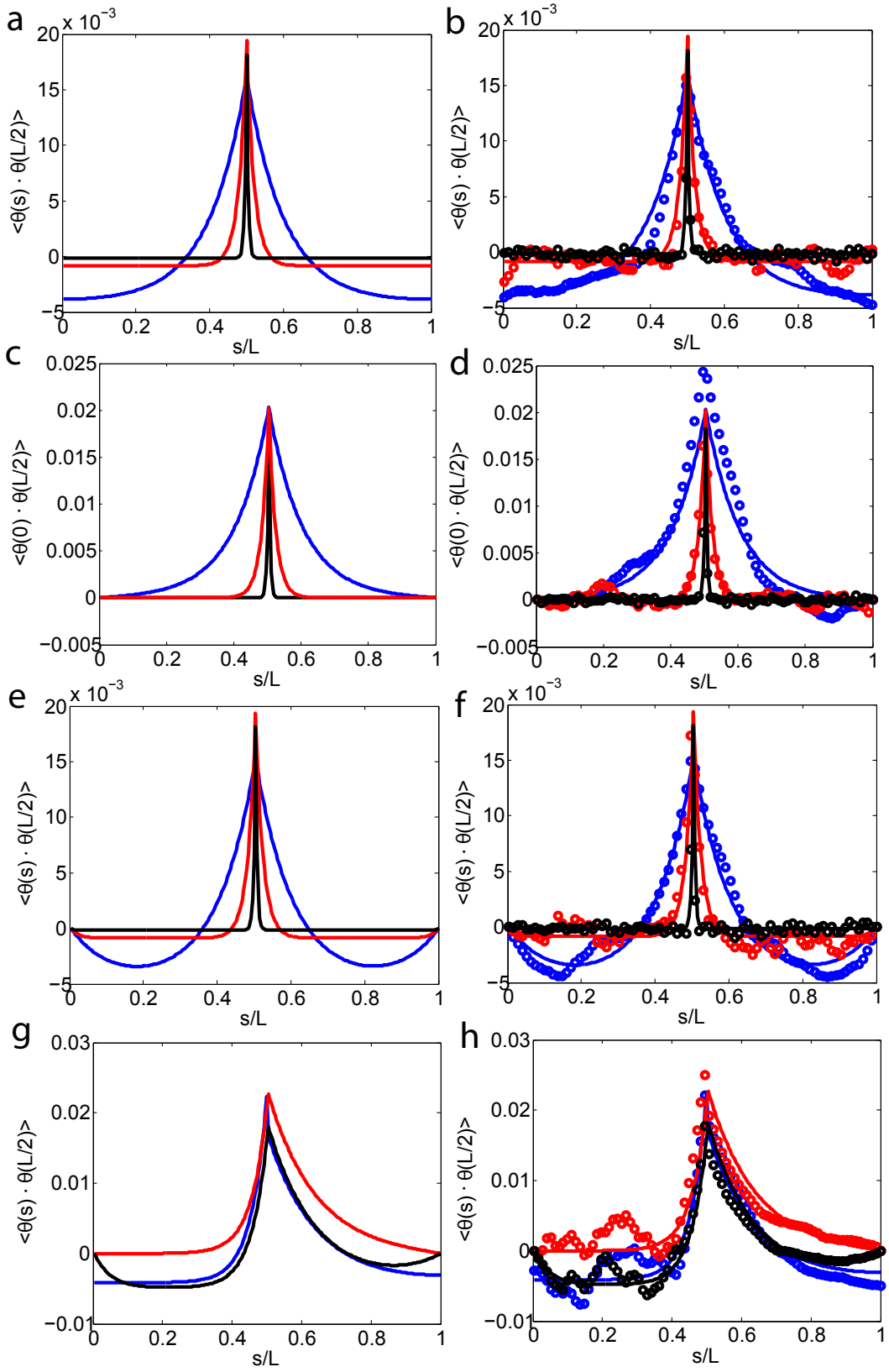

Figure 8:

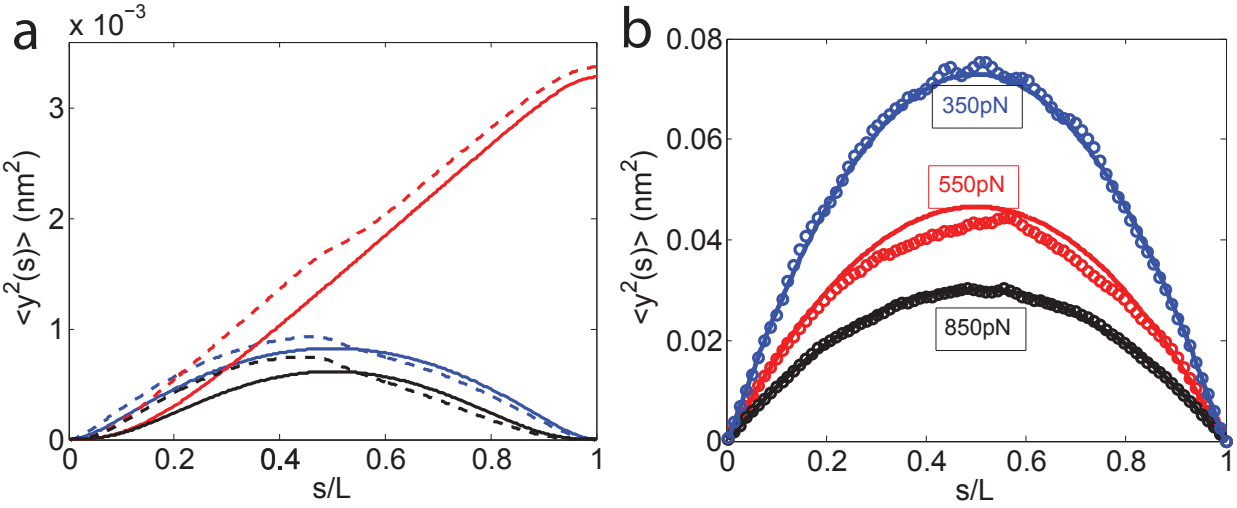

Figure 9:

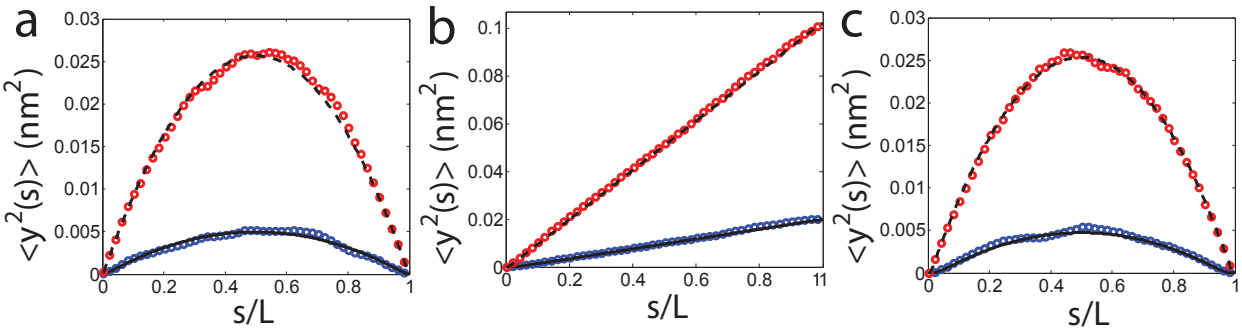

Figure 10:

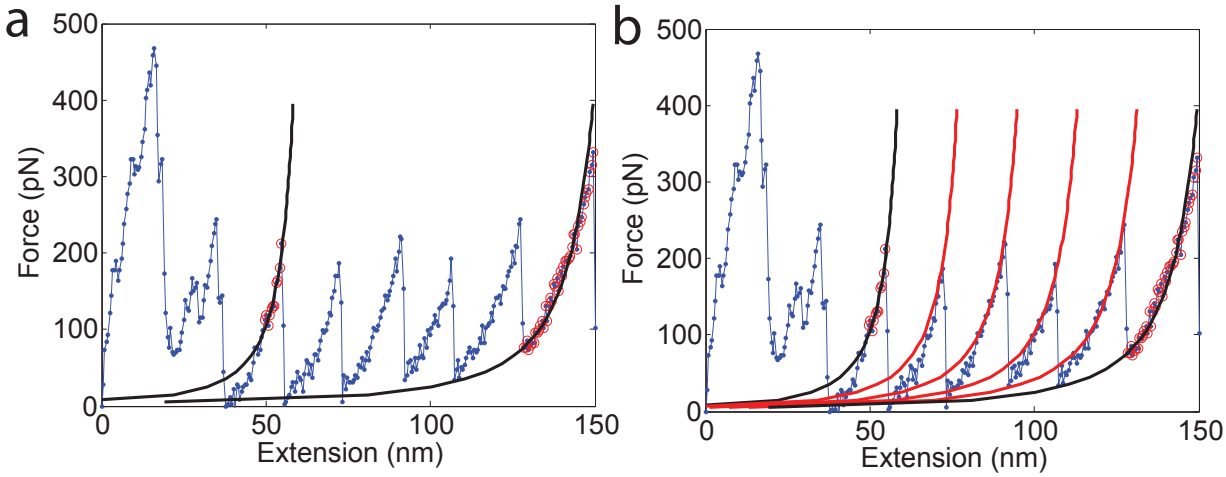

Figure 11: